ENGINEERING A SELF-TARGETING ENTRY INHIBITOR FOR MALARIA PROPHYLAXIS

by

Shuhao Xiao

A thesis submitted to Johns Hopkins University in conformity with the requirements for the degree of Master of Science

Baltimore, Maryland

April, 2019

Abstract

A critical step in *Plasmodium falciparum* (*Pf*) host cell invasion is the formation of a tight junction between the parasite and the host cell, which provides a firm anchor to facilitate parasite entry. This step requires interaction between the micronemal protein AMA1 and RON2, a component of the parasite secreted RON receptor complex. This interaction is also required for efficient *Pf* sporozoite invasion of hepatocytes. This is a unique example in host-pathogen interactions where both ligand and receptor are provided by the parasite for successful host cell entry.

We recently showed that a 49 amino acid region of RON2 (termed RON2L) is sufficient to bind AMA1 and block invasion, thereby acting as a potent entry inhibitor. RON2L and its binding pocket in AMA1 is conserved within each *Plasmodium* species and points to an evolutionarily preserved "lock-and-key" mechanism designed to prevent changes. We reasoned that targeting this interaction can be an effective antimalarial strategy as it would make it harder for the parasites to develop resistance. To do this, we are developing a novel gene therapy approach using adeno-associated virus (AAV) to endogenously express the entry inhibitor RON2L masked as a human Ig fusion protein (RON2L-Ig). We show that the entry inhibitor expressed by AAV transduction is produced as a correctly folded, stable fusion protein and potently neutralized *P. falciparum* merozoites *in vitro*. We are using a *in vivo* rodent malaria model and a *P. falciparum* humanized mouse model to evaluate protection against infection and disease. Our data indicate that self-targeting this critical invasion pathway used by both the transmitting and disease-causing forms of *Plasmodium* could provide an effective prophylaxis tool that can augment current malaria elimination efforts.

Acknowledgements

First and foremost, I would like to express my sincere gratitude to my advisor Dr. Prakash Srinivasan, who has been a fantastic mentor during the course of my thesis research. I am extremely fortunate to have the chance to work with Prakash side by side in the lab, and I cannot estimate how much time he has set aside to personally teach me how to perform the experimental techniques. Outside of the laboratory, his door is always open to me whenever I have doubts or questions. As a graduate student, it is truly a privilege for me to be able to work independently on such an exciting project, and I am grateful for the opportunity and trust Prakash has placed in me.

I would like to thank all members in the Srinivasan lab—Deepti, Maryam, Lyu Yi, Sophia, and Vani for their incredible support. I would also like to acknowledge the contribution of our former members—Rajeev and Cameron Bell, who laid the groundwork of this project before I joined the lab and made my job much easier, and Garima, who also provided many helps along the way. Working with such a brilliant group of individuals in the lab has been a wonderful experience for me, and I am thankful for what I have learned from them.

I would like to thank my secondary thesis reader Dr. Gary Ketner for his guidance in the AAV experiments as well as his invaluable feedback and suggestions on my thesis. I am also grateful for the assistance provided by his lab member Suk, who has been a very good partner in the virus preparation experiment.

Lastly, and certainly not least, I want to say that words are not enough to fully express my gratitude to my family. I would never be at where I am today without their unconditional love and support over the years.

Table of Contents

List of Figures

List of Tables

.

Introduction

Malaria is a life-threatening disease caused by *Plasmodium* parasites, and it is transmitted to people through bites of infected female *Anopheles* mosquitoes. In May 2017, World Health Assembly published the *Global Technical Strategy for Malaria 2016–2030* (GTS)[1] that provides a comprehensive framework to guide countries in their efforts to accelerate the progress towards malaria elimination. Despite of large amount of investment made every year, malaria continues to pose one of the greatest threats to public health. There were 219 million clinical cases and an estimated 435,000 malaria deaths in 2017, mainly in Sub-Saharan Africa[2]. Data also suggested that no significant progress in reducing global malaria cases was made during the past few years, although the number of deaths has been reduced by almost 30% comparing to 2010. GTS sets the goal of reducing global malaria incidence and mortality rates by at least 90% by 2030. However, to reach its 2030 target, it is estimated that annual malaria funding will need to increase to at least US dollar 6.6 billion per year by 2020.

Current strategies to prevent and treat malaria include the use of insecticide-treated mosquito nets (ITNs), global access to rapid diagnostic tests (RDTs), and employing artemisinin-based combination therapy (ACT) to treat patients. While malaria control strategies have shown promising outcomes, significant challenges remain to be overcome if we are to achieve the quickly approaching 2020 and 2025 GTS milestones. Global reports of 2010-2016 showed resistance to the four commonly used insecticide classes has been widely spread in all major malaria regions in the world[3,4]. Even more worryingly, multidrug-resistant strains, including artemisinin-resistant *P. falciparum*, started to emerge in recent years independently in different countries, and spread between countries in the Greater

Mekong Subregion (GMS)[5,6]. Hence, the lack of a vaccine and the emergence of resistance to front-line antimalarials warrant development of novel approaches to prevent malaria.

Plasmodium *life cycle*

Malaria parasite *Plasmodium* is an obligate, unicellular eukaryotic parasite and belongs to a large phylum of parasitic alveolates called *Apicomplexa*. Most Apicomplexans, including *Toxoplasma gondii*, *Plasmodium falciparum* and other *Plasmodium* spp. possess a unique form of organelle that comprises a type of plastid termed apicoplast, which hosts important metabolic pathways like fatty acid synthesis, isoprenoid precursor synthesis, and parts of the heme biosynthesis pathway[7]. Life cycle of *Plasmodium* parasites involves multiple distinct stages in the vertebrate and mosquito vector **(Figure 1)**[8]. When an infected mosquito takes a blood meal from a vertebrate host (e.g. human), *Plasmodium* sporozoites, the invasive forms that are present in the salivary gland of the insect, are injected into the dermis and stay there for at least thirty minutes[9]. Subsequently, the sporozoites enter the blood circulation and reach the liver, where they infect hepatocytes and undergo a large round of replication. At the end of intra-hepatic development thousands of merozoites are produced from each infected cell[10]. The released merozoites immediately infect erythrocytes and initiate the blood-stage infection cycle. Generally, it takes parasites 24-72 hours (depending on the species) to undergo the asexual replication in red blood cells (RBCs). Inside RBCs, the parasites transform from rings to trophozoites, and finally mature to schizonts containing 16-32 merozoites, which are soon released following erythrocyte lysis. While the parasites go through continuous cycles of erythrocyte infection in the host blood stream, some will differentiate into sexual erythrocytic stage parasites, known as gametocytes. When both male (microgametocytes) and female (macrogametocytes) are ingested by a mosquito

during a blood meal, together they will go through the sporogonic cycle in the mosquito gut, resulting in the development of innumerable sporozoites that will finally migrate into the salivary gland of the mosquito and await for the next injection into vertebrate host and thus continuing the cycle[11].

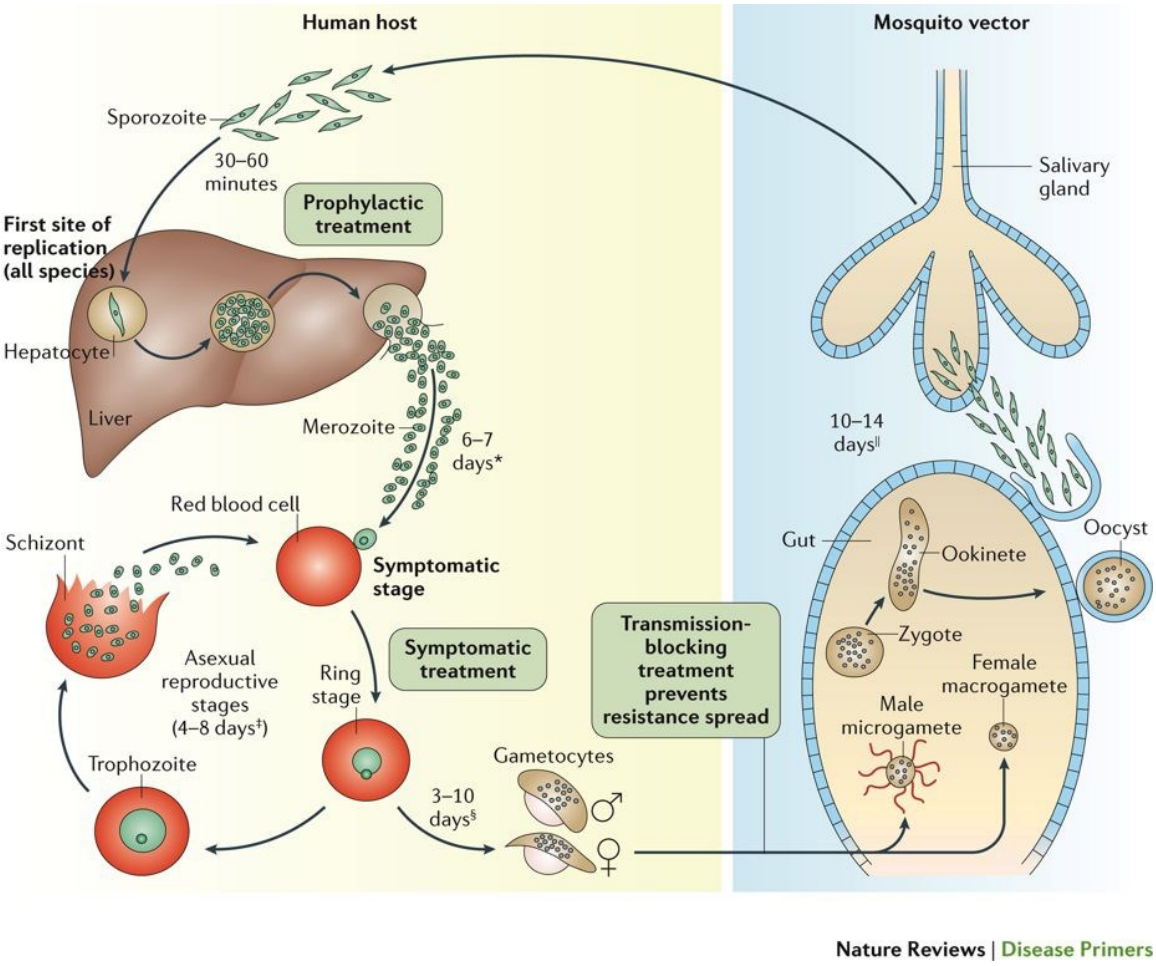

Figure 1. *Plasmodium* parasite life cycle.

Parasite invasion and the interaction between AMA1 and RON2

Comprehensive understanding of parasite invasion mechanism can lead to discovery of drugs that effectively block the entry process of the parasite thus prevent malaria clinical symptoms, and more importantly, the massive number of replications in the host that cause

disease transmission. Electron microscopy studies have identified unique secretory organelles, such as the dense granules, micronemes, and rhoptries, located at the *Plasmodium* merozoite apical end and storing essential molecules for parasite egress and invasion (**Figure 2**). These molecules mainly belong to two families–erythrocyte binding-like (EBL) and reticulocyte binding-like homologues (Rh), respectively localizing to the micronemes and rhoptry neck[12–16]. Key event of the invasion process is the release of these molecules from the secretory organelles so that they can interact with host cell receptors and initiate entry process. Once merozoites are released from the infected RBCs, they are exposed to a low-potassium level environment, which triggers the calcium efflux from the endoplasmic reticulum (ER) and the translocation of microneme contents to the merozoite surface[17]. Invasion of *Plasmodium* spp. merozoites begins with an initial weak attachment, followed by an active process of reorientation that ultimately brings the apical end of the parasites into close apposition with the RBC surface[18,19]. Consequently, this event triggers the formation of a moving junction, which can be observed by transmission electron microscope (TEM) manifesting as a dense region under the cytoplasm of RBC; meanwhile the merozoite secretes its rhoptry contents that facilitate the invasion process[20]—having the moving junction as a firm anchor for entry, the parasite actin-myosin motor drives the cell motility and pull the merozoite into the RBC[21].

Among all the identified invasins to date, apical membrane antigen 1 (AMA1) is considered as one of the most promising targets for vaccine and therapeutics development due to its critical role in parasite's invasion process[22–24]. AMA1 is a protein initially localized inside micronemes of the parasite in the form of an 83 kDa precursor[25,26], and later translocated onto the surface in a 66 kDa form by the time of schizont rupture and release of

merozoites[27,28]. AMA1 is unique to Apicomplexan parasites and derives from a single essential gene present in all *Plasmodium* species[29]. Immunoprecipitation experiment of AMA1 in the parasite detergent extracts identified a complex of rhoptry neck proteins (RONs)[30,31]. Interestingly, RON complex appears to be secreted by the parasite into and translocate across the RBC membrane, where it serves as the receptor for AMA1[32]. RON2 is found to be the only transmembrane protein in the RON complex that interact directly with AMA1 by inserting its second and third hydrophobic helices into the hydrophobic pocket of AMA1 (**Figure 3**)[32–38]. Recently, the interaction between AMA1 and RON2 has been found to be critical for triggering junction formation, and it depends on the presence of two conserved Cys residues within the RON2 sequence between the second and the third hydrophobic helices, termed RON2L[32]. It was also shown that unlike other steps where functionally redundancy exists, the junction formation induced by the interaction between AMA1 and RON2 in *Plasmodium* spp. has no alternative pathways[32]. The same study also showed that the number of invasion event was significantly reduced by having the short peptide RON2L in the parasite culture. Importantly, RON2L and its binding site on AMA1 are both conserved among all *Pf* genetic variants[33,34]. In addition, studies have confirmed that such invasion mechanism is also shared in pre-erythrocytic stage parasite invasion process, and a RON2L-like molecule was shown to have an inhibitory effect on sporozoite invasion into hepatocytes[39,40]. These evidences point at a functional constraint governing an essential step in parasite invasion and represent a novel target can potentially be exploited for antimalarial therapy.

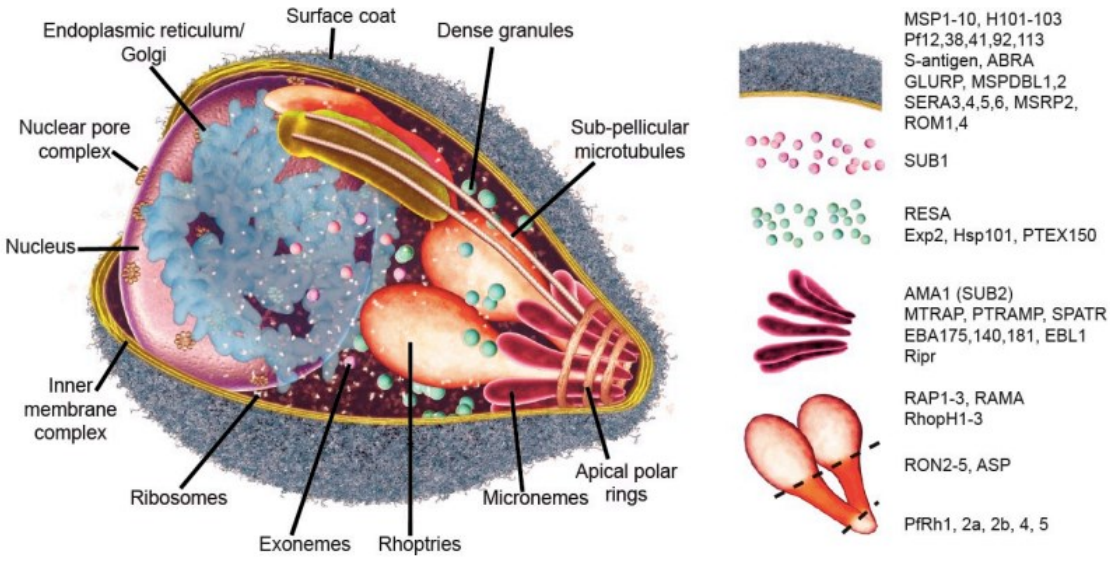

Figure 2. Crucial organelles and molecules for merozoite invasion. Important molecules for parasite invasion and their corresponding locations are listed on the right.

AMA1-RON2 as anti-malarial target

Evidence of AMA1 polymorphism has been reported since 1990[41]. One of the most striking evidence is that a single trial site in Mali identified strikingly 214 AMA1 variants in total among 506 subjects, indicating an extreme sequence diversity of AMA1[42]. Immune responses have been thought to be the predominant selective factor for the mutations, hence also has encouraged a belief that immune responses to AMA1 can indeed have a parasite-inhibitory effect in humans[43]. AMA1 has been a leading blood-stage malaria vaccine candidate, however, its polymorphism continues to be the greatest obstacle towards the development of a successful vaccine. To date, two phase 2 trials have been conducted to measure the protective effect of AMA1 vaccines, but both showed either no significant efficacy or only average protection against vaccine-type parasites[44,45].

Discouraged by the vaccine trial results, alternative methods that target AMA1-RON2 interaction has been sought. Recent vaccination studies using a pre-formed AMA1-RON2L complex instead of individual antigens in a mouse malaria model showed great protection against a highly virulent *Plasmodium yoelii* YM parasite. Antibodies induced after vaccination of the complex showed an increased inhibitory activity largely due to distinct target sites on new AMA1 epitopes surrounding the RON2-binding pocket[46]. A follow-up study showed the complex vaccine in Freund's adjuvant also provided protection in *Aotus* monkeys against a virulent *P. falciparum* infection[47]. In addition, small molecules that can block AMA1-RON2 interaction were identified by screening a library of over 21,000 compounds[48], providing an additional path towards malaria treatment.

Neutralizing antibodies and their coordinating Fc-receptors play key roles in malaria therapeutics[49]. Natural antibodies elicited by AMA1 vaccines often target the highly polymorphic region of the protein thus the parasite can easily evade antibody neutralization through mutation and evolution[50,51]. Here we aim to design an antibody-like inhibitor which can competitively bind to the conserved region of the invasion ligand AMA1 thus block parasite invasion. To do this, we utilize the binding peptide RON2L which, as described above, insert itself into the conserved hydrophobic pocket of AMA1. We replaced the variable regions on both the light and heavy chains of a human IgG1 antibody with RON2L peptide, resulting in a tetravalent inhibitor which, henceforward termed "RON2L-Ig", can potentially bind to four AMA1 molecules at the same time. It is called "self-targeting" due to the fact that RON2L is a parasite-originated peptide that binds to the parasite ligand AMA1. We reason that the human immunoglobulin (Ig) which has a relatively large size (~150 kDa) can mask the foreign peptide RON2L, thus preventing the inhibitor from inducing an

immune response. We also reasoned that in addition to the direct blocking effect, once tagged by the inhibitor, parasites can be efficiently engulfed and processed by antigen presenting cells (APCs) with receptors that recognize the Fc region of the inhibitor, and potentially further leads to a therapeutic vaccination effect. Additionally, previous studies have shown that the Fc region on the human IgG facilitates clearance of parasites through antibody-dependent cellular cytotoxicity (ADCC)[52,53], a mechanism of cell-mediated immune defense whereby an effector cell of the immune system (e.g. monocytes) actively lyses a target parasite by recognizing the Fc region of the antibodies binding to the membrane-surface antigens. Finally, Fc region of the inhibitor may also recruit C1q from complement system and activate complement fixation, ultimately leading to parasite lysis[54].

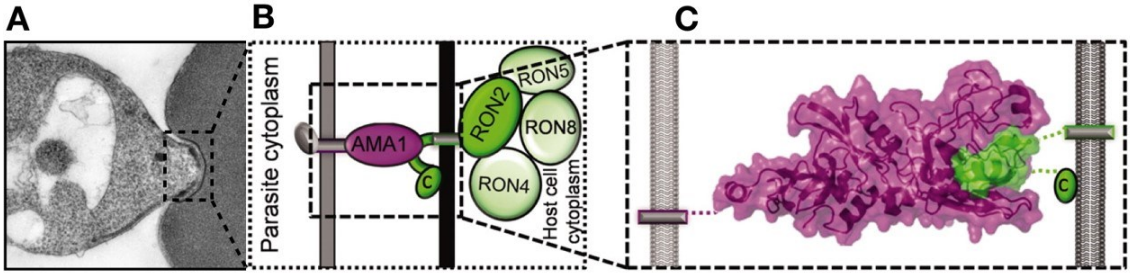

Figure 3. Illustration of AMA1-RON2 interaction. (**A**) Apical end of the parasite in close contact with RBC surface, and a dense region under the RBC cytoplasm can be observed. (**B**) AMA1 interaction with RON complex at the interface between parasite and host cell. (**C**) Note that only the ectodomain of the RON2 protein interact directly with AMA1 by inserting itself into the hydrophobic pocket of AMA1.

Adeno-associated viral vector for malaria prophylaxis

The most common viral vector that has been employed in gene therapy studies and clinical trials is adeno-associated virus (AAV), a nonenveloped virus from *Parvoviridae* family that infects humans and other primate species. AAV is replication-defective in the absence

of helper viruses, such as adenovirus and herpes simplex virus[55,56]. Currently no known disease is reported to be caused by AAV apart from a very mild immune response[57]. So far it has been discovered that AAV has as many as 11 serotypes with distinct tropism towards various cell types—serotypes 2, 3, 5, and 6 infects human cells, while the rest are found to infect nonhuman primates[58]. In contrast to the wild-type virus, recombinant AAV enters human and nonhuman primate cells and persists in an extrachromosomal state without integration into host cell genome, although a low frequency of random integration that leads to genetic toxicity has been reported[57,59,60]. Multiple AAV-based gene therapies are being tested in clinical trials, including Hemophilia[61], congestive heart failure[62], Parkinson's disease[63]. The first AAV-based gene therapy licensed in the world is Alipogene tiparvovec (Glybera) that is used to treat lipoprotein lipase deficiency (LPLD)[64,65]; while in the U.S., it is not until the beginning of last year that the first AAV-based gene therapy called LUXTURNA™ by Spark Therapeutics was approved for treating inherited blindness disorder biallelic RPE65 mutation-associated retinal dystrophy[66].

An alternative option to immunization is viral vector-mediated passive delivery of effector genes (e.g. pathogen-specific antibodies). Such technique is called vectored immunoprophylaxis (VIP), and was first pioneered by Johnson *et al.* in 2009, where it was showed that AAV-delivered immunoadhesins could protect most rhesus macaques from a simian immunodeficiency virus SIVmac316 challenge[67]. Subsequent studies using AAV-mediated *in vivo* expression of monoclonal antibodies reported high level antibody production which is maintained for several months after a single intramuscular injection, and protected humanized mice and macaques against HIV, influenza A virus, and transgenic *Plasmodium*

parasite[68–71]. On the other hand, AAV has also been employed to deliver artificially designed inhibitor drugs for blocking pathogen entry. For example, inhibitor drug eCD4-Ig comprising of domains 1 and 2 of the CD4 receptor and a small CCR5-mimetic sulfopeptide together fused to a human IgG1 Fc domain was shown 100% neutralization efficiency of a diverse panel of neutralization-resistant HIV-1, HIV-2, and SIV isolates, including a comprehensive set of isolates resistant to the CD4-binding site bNAbs VRC01, NIH45-46 and 3BNC117; when delivered by an AAV vector, the drug eCD4-Ig provided a great protection from SHIV infection in non-human primate model[72]. Moreover, a strong ADCC effect was observed by following studies, suggesting an additional protection effect contributed by the Fc region of the inhibitor[73,74].

Here we propose to employ AAV vector to deliver the gene of our inhibitor RON2L-Ig for malaria prophylaxis. We aim to first engineer a recombinant AAV that is used for transducing animals and inducing *in vivo* expression of the *Plasmodium* entry inhibitor RON2L-Ig. WE expect that this will result in durable, systemic expression of stable inhibitor from rAAV transduced muscle cells. Upon challenge with blood-stage malaria parasites, RON2L-Ig present in circulation is expected to bind to AMA1 on the surface of merozoites, preventing them from engaging with *Plasmodium* secreted RON2 receptor on host cells, thereby neutralizing parasites before their invasion into RBCs. In addition, upon sporozoite challenge through infected mosquito bite, RON2L-Ig is expected to also bind to AMA1 on the sporozoite surface and preventing the parasite from reaching and infecting the hepatocyte. The dual mode of action of this *Plasmodium* self-targeting entry inhibitor could therefore prevent both infection as well as confer protection against disease.

Material and Methods

Construction and cloning of pcDNA™3.1-PfRON2L-Ig and pAAV-Py-RON2L-Ig

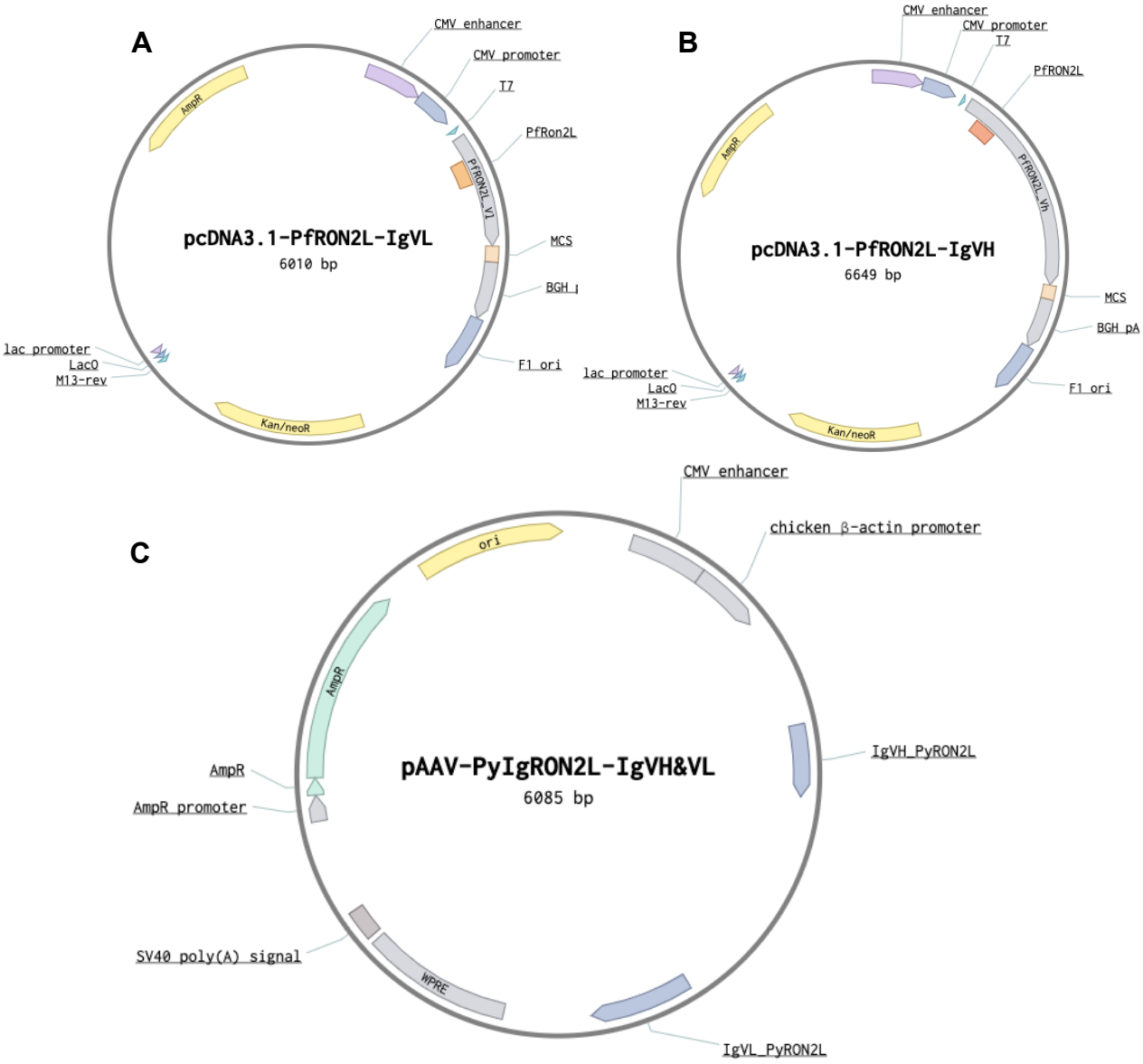

Figure 4. Plasmid maps of (**A**) pcDNA™3.1-*Pf*RON2L-IgV$_L$, (**B**) pcDNA™3.1-*Pf*RON2L-IgV$_H$, and (**C**) pAAV-*Py*RON2L-Ig-V$_H$V$_L$.

To express b12 (anti-HIV-1 gp120) and 2A10 (anti-*P. falciparum* CSP) antibodies in mice, their DNA sequences of the variable regions were synthesized based on published sequences and cloned into the VIP expression vector as previously described[68,71]. This was done in Dr. David Baltimore's laboratory at California Institute of Technology by Dr. Alejandro Balazs and tested further by Dr. Cailin Deal in Dr. Gary Ketner's laboratory at Johns Hopkins Bloomberg school of Public Health. These previously studied VIP expression vector plasmids were used in this study as controls. For engineering the VIP vector that expresses the gene of our inhibitor used in rodent model, 2A10 antibody variable regions on both heavy and light chains were replaced with synthesized *Py*RON2L from published sequence (**Figure 5**)[32]. The 2A10 heavy chain variable region was removed by digesting the plasmid with NotI and SacI restriction enzymes at 37 °C overnight, then Gibson Assembly was performed by adding synthetic *Py*RON2L-Ig_V_H insert at 3:1 ratio into the gel purified double digested pAAV at 50 °C for one hour. 2A10 light chains were replaced with synthetic *Py*RON2L-Ig_V_L insert following the same process. After excising the variable region of 2A10 heavy and light chains and substituting the RON2L sequence, 30 seconds of heat-shock transformation at 42 °C using XL10-Gold® Ultracompetent Cells was performed. Following transformation, cells were plated on prewarmed LB agar plates with 100 μg/mL ampicillin for selection, and the plates were incubated at 37 °C overnight. On the next day, positive clones were identified by colony PCR. ZymoPURE™ II Plasmid Midiprep Kit was used to purify plasmid DNA from 1 L of bacteria culture, and the concentration of the plasmids were measured using NanoDrop™ 1000 Spectrophotometer.

To produce inhibitor for *in vitro* characterizations, 2A10 antibody variable regions on both heavy and light chains were replaced with synthesized *Pf*RON2L from published sequence[32], then the entire *Pf*RON2L-IgG_V_H-*Pf*RON2L-IgG_V_L region was cut off from the VIP vector and inserted into a pcDNA™3.1 vector. pcDNA™3.1 vector purchased from Thermo Fisher Scientific contains a cytomegalovirus (CMV) enhancer-promoter for high-level expression, a large multiple cloning site in either forward (+) or reverse (–) orientations, a Bovine Growth Hormone (BGH) polyadenylation signal and transcription termination sequence for enhanced mRNA stability, a SV40 origin for episomal replication and simple vector rescue in cell lines expressing the large T antigen, and Ampicillin resistance gene and pUC origin for selection and maintenance in *E. coli*. This vector was chosen due to its optimal performance in transfection of mammalian cell lines. Maps of the plasmids described above are shown in **Figure 4**.

To increase the flexibility of the inhibitor, a Gly-Gly-Ser-Gly linker was added between the RON2L peptide and C_H1 of the heavy chain or C_L of the light chain. Gly and Ser were used because of their small sizes that allow flexible movement, while at the same time Ser helps maintain stability of the structure through formation of hydrogen bonds with water molecules thus avoid undesired interactions[75,76]. In addition, signal sequence (SS) was added to 5' end of both heavy and light chain. Signal peptides are important for transporting newly synthesized proteins from ER to cell exterior across membrane, and experiments showed that mutations in the signal peptide sequence resulted in decrease in the secretion efficiency of the antibody[77]. These features are shown in the schematic representation of the VIP expression vector in **Figure 5**.

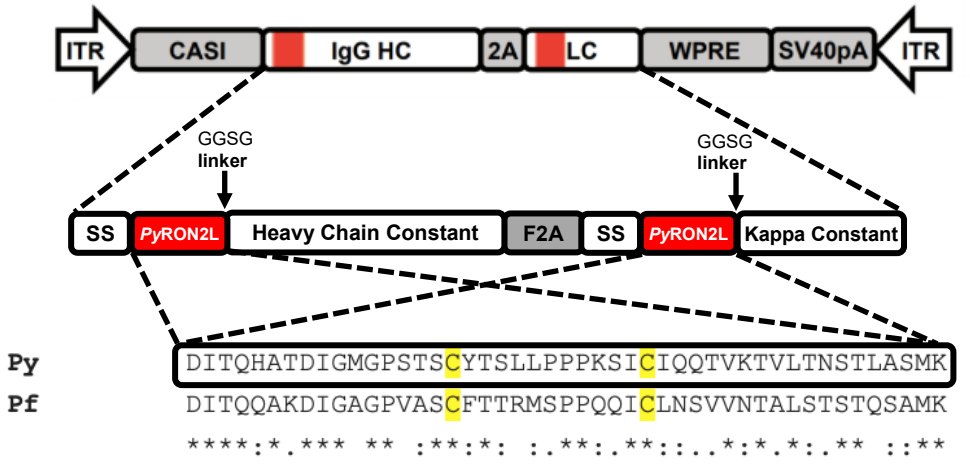

Figure 5. Schematic representation of VIP expression vector.

Production, purification, and quantification of inhibitor

To begin with, frozen Human Embryonic Kidney 293T cells (previously preserved in freezing medium composed of 90% complete medium and 10% DMSO) were thawed and cultured in a 5% CO_2 incubator at 37 °C in complete medium (Dulbecco's Modified Eagle's Medium, 10% fetal bovine serum). After confluency reaches 70-80%, cells were transfected with pcDNA-*Pf*RON2L-Ig_V_H and pcDNA-*Pf*RON2L-Ig_V_L at 1:1 ratio mixed with jetPRIME reagent and buffer according to manufacturer's protocol[78]. For each T175 flask, 10 µg of plasmid in total, 1.25 mL of jetPRIME buffer, and 50 µL of jetPRIME reagent were mixed and added to the culture medium. Cell culture supernatant was collected every 48 hours and filtered (Millipore) after adding protease inhibitor, then stored at 4 °C.

Two different methods, ammonium sulfate precipitation and sodium sulfate precipitation, were tested first to compare their efficiency. Saturated ammonium sulfate solution was prepared by adding excess solid $(NH_4)_2SO_4$ to distilled water (about 950 g to 1 L) and stirred overnight at room temperature. This solution (in contact with solid salt) was stored

at 4 °C for use. Saturated ammonium sulfate solution was added drop-wise into the supernatant collection to produce 50% final saturation and stirred at 4 °C overnight. On the next day, solution was centrifuged at 4,000 rpm for 1 hour at 4 °C. The supernatant was discarded, and remaining liquid was drained by carefully inverting the tube over a paper tissue. For sodium sulfate purification, solid Na_2SO_4 was added to produce an 18% w/v solution (i.e., add 1.8 g/10 mL), and stirred at 25 °C for 30 minutes to 1 hour. Next, the solution was centrifuged at 4,000 rpm for 1 hour at 25 °C. The supernatant was discarded, and the pellet was drained on a paper tissue. Finally, after finishing either method, the pellet was dissolved in PBS in 10% volume comparing to that of the original supernatant and can be stored at 4 or −20 °C until affinity purification.

To purify the modified IgG, equal volume of IgG binding/washing buffer (G-Biosciences) was added and mixed with PBS dissolved pellet. Protein G column was equilibrated with 30 mL of IgG binding/washing buffer at room temperature, then the 1:1 diluted solution was added on to the column and let flow through by gravity. Next, the column was washed with 10 mL of IgG binding/washing buffer again, followed by elution using 5 mL of IgG elution buffer (G-Biosciences) into a 30 kDa filtration tube containing 150 µL of pH 9.0 Tris-HCl for neutralization. The inhibitor protein went through multiple rounds of dialysis by centrifuging at 4 °C 4,000 rpm to replace the buffer with incomplete RPMI. Finally, the inhibitor protein in incomplete RPMI was sterile filtered through a 0.22 µm filter unit and kept at 4 °C.

Inhibitor characterization

Purified RON2L-Ig was loaded on an SDS-PAGE protein gel at 100V for 1 hour. The protein gel was washed in water for four times to remove SDA, then stained with Coomassie blue for 2 hours. For western blot analysis, the SDS-PAGE gel was transferred to a methanol-activated PVDF membrane using an Invitrogen Power Blotter at 1.3 Amp for 10 minutes. Next, the PVDF membrane was blocked with Thermo Fisher Scientific SuperBlock Blocking buffer and 0.1% TWEEN 20 on the shaker overnight. The next day, secondary antibody (Alkaline phosphatase conjugated anti-human IgG antibody) was diluted in blocking buffer 1:2,500 and incubated with membrane at 4 °C on the shaker for 2 hours. Subsequently, the membrane was repeatedly washed with wash buffer (1× PBS and 1% TWEEN 20) for 10 minutes. 1 mL of West Blue® Stabilized Alkaline Phosphatase substrate for was added to the membrane, and the reaction was neutralized by washing with distilled water.

For quantification of human IgG expression level, standard enzyme-linked immunosorbent assay (ELISA) was performed (**Table 1**). 0.02 μg of goat anti-human IgG-Fc antibody (Bethyl) was added into each well of the plate and incubated overnight at 4 °C. The next day, plate was blocked with 200 μL blocking buffer (1% BSA Sigma in 1× PBS and 0.1% TWEEN 20) per well for 1 hour. Meanwhile samples were four-fold serially diluted in blocking buffer on a clean 96-well plate. 100 μL of each sample dilution was transferred to the ELISA plate and incubated for 1 hour at room temperature. Plate was then washed for four times with wash buffer (1× PBS and 0.1% TWEEN 20) and incubated with 100 μL per well of HRP-conjugated goat anti-human kappa light chain antibody (Bethyl) 1:10,000 diluted with blocking buffer for 1 hour at room temperature. Plate was washed

again four times, then 100 µL of TMB Super Sensitive 1-Component HRP Microwell Substrate was added into each well. The plate was incubated in the dark for 2 minutes at room temperature, followed by neutralization with 100 µL Stop Solution for TMB Substrates. Plate was read at a wavelength of 450 nm using a microplate reader. A standard curve was generated based on the reading of Human Reference Serum (Bethyl), and OD data of the samples were interpolated using the standard curve to calculate hIgG concentration.

For characterizing inhibitor's binding activity against AMA1 molecule, ELISA plates were coated with 0.1 µg of *P. falciparum* recombinant AMA1 molecule per well overnight at 4 °C. Other steps were performed as described above. *Pf*RON2L-Ig_V_H and V_L, 1:2,500 diluted anti-human Alkaline Phosphatase conjugated anti-hIgG (H+L) secondary antibody was used for detection, followed by adding Sigma-Aldrich Phosphatase substrate and read at 405 nm wavelength using a microplate reader. ELISA coating and primary reagent specifications are summarized in **Table 1**.

ELISA target	**Analyte**	**Coating reagent**	**Analyte Starting Dilution**
hIgG	Human Reference Serum (HRS) standard; hIgG	Anti-human IgG-Fc region antibody	Cell culture supernatant: 1/1; Mouse sera: 1/5,000; HRS: 2 ug/mL; Precipitated protein: 1/50; Protein G column purified: 1/1,000
*Pf*RON2L-Ig	Cell culture supernatant and purified protein	*Pf*AMA1 molecule	Precipitated protein: 1/5; Protein G column purified: 1/1,000
Mouse anti-RON2L-Ig	Mouse sera	*Py*RON2L molecule	Mouse sera: 1/5,000;
Mouse anti-hIgG	Mouse sera	hIgG	Mouse sera: 1/5,000;

Table 1. Coating and primary reagent specifications for ELISA.

Immunofluorescent assay (IFA) was performed to confirm that RON2L-Ig inhibitor could bind to its natural AMA1 ligand in the parasite. *P. falciparum* infected blood smears were made from parasite culture containing mature schizonts. Fixative solution (2.5% PFA, 0.1% GA, 3% sucrose) was added to the slides and incubated for 10 minutes, then aspirated with vacuum, following by washing with 1× PBS for 3 times. Next, blocking buffer (1× PBS, 2% BSA, 0.1% Triton X-100) was added on the slides and incubated for 1 hour at room temperature. Purified inhibitor *Pf*RON2L-Ig diluted 1:100 in blocking buffer was added to the slides, then gently covered with a coverslip (to avoid the coverslip contacting the smears). The slides were incubated at 4 °C overnight. On the next day, the slides were washed with wash buffer (1× PBS and 0.1% Triton) for 5 times. Secondary antibody (488 goat anti-human antibody) 1:200 diluted was added to the slides and kept in dark for 2 hours, then washed with wash buffer. Finally, 5 µL of ProLong™ Gold Antifade Mountant mounting solution was added to the smears and mounted with coverslips. Anti-AMA1 antibody (1:1000 dilution) was added to confirm co-localization with *Pf*RON2L-Ig. Anti-rabbit Alexa Fluor® 633 was used on secondary antibody.

Finally, growth inhibitory assay was performed to demonstrate that the inhibitor was capable of neutralizing parasite *in vitro* and preventing its invasion into RBCs. 1 L of complete media (CM) was prepared by adding 5 g of Albumax, 30 mL of $NaHCO_3$, and 2.6 mL of gentamycin into 967.4 mL of Roswell Park Memorial Institute (RPMI) 1640 Medium. To do this, parasites were first synchronized at late schizont stage by Percoll/sorbitol synchronization method as previously described[79]. Briefly, 90% Percoll with 6% sorbitol was prepared by adding 12 g of D-Sorbitol into the mixture of 20 ml of 10× RPMI-HEPES and

180 ml of Percoll. 70% Percoll-sorbitol was prepared by mixing 37.5 mL of 90% Percoll/6% soribitol solution with 10.5 mL of 1× RPMI-HEPES. 40% Percoll-sorbitol was prepared by mixing 21 mL of 90% Percoll/6% sorbitorl solution with 27 mL of 1× RPMI-HEPES. Gradients were prepared into a 17×100 mm tube, starting with 70% Percoll/sorbitol and overlaying with the others in sequence of 3 mL of 70% Percoll/sorbitol, 3 mL of 40% Percoll/sorbitol, then 1-2 mL of parasite solution. Gradients were centrifuged at 10,000 rpm for 20 min at RT, then parasitized RBCs at the interface between 40% and 70% Percoll/sorbitol were collected and transferred to a new 50 mL tube. Incomplete media was added dropwise to the parasitized RBCs, then centrifuged again at 400 g. Lastly, cells were washed with the same volume of incomplete media (iCM) and finally cells were resuspended in 1 mL of CM.

Parasitemia of the synchronized parasite culture was calculated by counting the proportion of parasite-infected RBCs on a prepared blood smear slide under light microscope. Accordingly, parasite culture was diluted to 0.5% parasitemia by adding additional 2% hematocrit CM. The parasite culture was collected in a 15 mL tube and centrifuged at 2,500 RPM for 5 min, then the media was removed and replaced with equal volume of 2× CM. Inhibitor protein was serial diluted with iCM on a half-area 96-well plate, then equal volume of parasite culture in 2% hematocrit 2× CM was added to each well. Consequently, each well contained 0.5% parasitemia 1% hematocrit 1× CM. E64D (50 μM) and EGTA (4 mM) were used as positive control. At the end of 48 hours, 5 μL of the completely resuspended parasite culture was taken from each well of the plate and mixed with 40 μL staining solution (1× PBS, 1:10,000 dilution of SYBR Green, and 1:10,000 dilution of MitoTracker) by constantly shaking in dark for 30 min. Subsequently, 200 μL of 1× PBS was

added to each well and mixed by shaking. At least 10,000 cells from each sample were run in the Invitrogen™ Attune™ NxT Flow Cytometer to detect cell fluorescence.

Production and purification of AAV-PyRON2L-Ig recombinant virus

Triple-plasmid transfection is the most common approach to generate recombinant AAV (**Figure 6,** adopted from SignaGen® website)[80,81]. The AAV genome is a molecule of single-stranded DNA of approximately 4.7 kb, with inverted terminal repeats (ITRs) that form T-shaped, base-paired hairpin structures at either end. Between ITRs at both ends are two genes (*rep* and *cap*) encode for four nonstructural proteins required for replication (Rep78, Rep68, Rep52, and Rep40) and three structural proteins that make up the capsid (VP1, VP2, and VP3). For the purpose of efficiently producing recombinant AAV, the *rep* and *cap* genes are deleted from the viral genome and provided in trans on a separate plasmid. The gene of interest is cloned into an expression plasmid flanked by the AAV ITRs. Genomic elements originated from adenovirus, including E1A, E1B, E2A, E4, and VA RNA region, are identified to be essential for AAV replication. Since HEK293T cell stably expresses the E1A and E1B proteins, only E2A, E4, and VA RNA region are included in the helper plasmid[82].

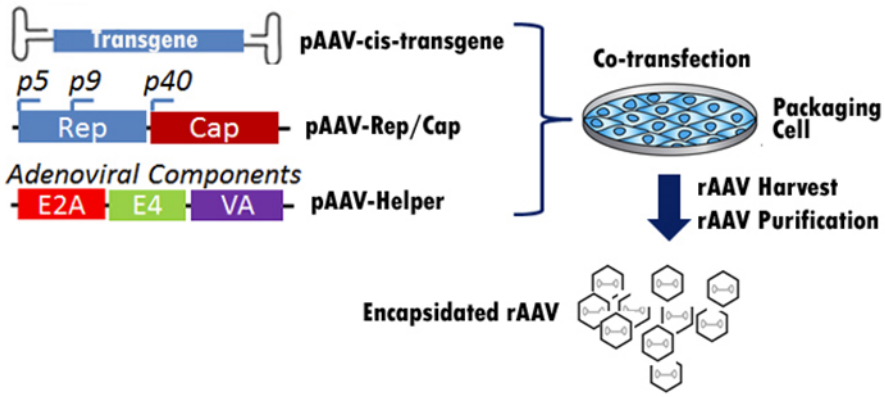

Figure 6. Triple-plasmid transfection for recombinant AAV production.

The method followed to prepare AAV vector virus expressing the 2A10 mAb has been previously described[71]. Briefly, three days before transfection, four 15 cm plates were seeded with 3.75×10^6 HEK293T cells each in 25 mL of DMEM and these plates were maintained in a 5% CO_2 incubator at 37 °C. Approximately 2 hours before transfection, the media in the plates were removed and replaced with 15mL of fresh DMEM containing 10% FBS, 1% P/S and 1% L-Glu (referred to as complete DMEM or cDMEM). 197 µg of AAV8 *rep* & *cap* DNA, 98.4 µg of helper vectors pHELP DNA (Applied Viromics) and 24.6 µg of pAAV-*Py*RON2L-Ig plasmid DNA were mixed together in a 50 mL tube. Then 16 mL of complete DMEM, 240 µL BioT was added and vortexed. The DNA was mixed with BioT and cDMEM mixture, vortexed and incubated for 5 min at room temperature, then 4 mL of this mixture was added to each 15 cm plate. The supernatant was collected and replaced with 15 mL fresh cDMEM media at five time points after transfection (36, 48, 72, 96, and 120 hours post-transfection). The supernatant was passed through a 0.22 µm filter (Millipore) and stored at 4 °C. At the end of the fifth collection, 75 mL of 5× PEG solution (40% polyethylene glycol, 2.5 M NaCl) was added to approximately 300 mL of supernatant. The virus in the supernatant was allowed to precipitate on ice for 24 hours at 4 °C. After precipitation, the solution was centrifuged (Sorvall RC5C centrifuge) at 5,000 RPM for 30 min at 4 °C, then the supernatant was discarded. The pellets were resuspended in 1.37 g/mL CsCl solution and then transferred to two Sorvall quick seal tubes. To form a gradient, the solution was centrifuged (Sorvall WX ultracentrifuge) at 60,000 RPM for 24 hours at 20 °C. Fractions (100-150 µl per well) were collected in a 96 well flat bottom plate, and refractive index of each of these fractions were determined using a refractometer. Fractions with a refractive index between 1.3755 and 1.3655 (which contained rAAVs)

were combined and the final volume was made up to 15 mL by adding Test Formulation Buffer 2 (TFB2, 100 mM sodium citrate, 10 mM Tris pH 8). The solution was pipetted on to a 100 kDa MWCO centrifugal filter (Millipore) and centrifuged at 4,000 RPM (Sorvall legend RT series centrifuge) at 4 °C for 30-45 min or till the retentate was below the 1 mL mark. This step was repeated for five times to wash the virus, each time adding 15 mL of TFB2 to the filter and repeating centrifugation. The membranes were washed with 300 µL of TFB2 and the final retentate was aliquoted and stored at −80 °C.

rAAV quantification

The unknown AAV virus and standard sample (AAV8 virus expressing b12 mAb-1×10^{12} GC/mL) were diluted tenfold in DNase buffer and 10 units of DNas I (Roche) was added to each sample. The samples were incubated at 37 °C for 30 mins. The Unknown AAV samples were diluted in DPEC treated water to 1:1,000, 1:10,000 and 1:100,000. The standard curve was created by diluting the standard sample four-fold in DPEC treated water from 2×10^{10} GC/mL to 0 GC/mL. A PCR mix containing 8.2 µL of SYBR green, 2 µL of DPEC treated water and 0.33 µL of forward and reverse primers (5' CMV: AACGCCAATAGGGACTTTCC and 3' CMV: GGGCGTACTTGGCATATGAT) or the luciferase transgene (5' Luc: ACGTGCAAAAGAAGCTACCG and 3' Luc: AATGGGAAGTCACGAAGGTG) per sample was prepared. 10 µL of PCR mix and 5 µL of sample were added to the 96-well PCR plate. The samples were run in duplicates in the MicroAmp Fast Optical 96-Well Reaction Plate. The copy number of rAAV in the samples were quantified using a quantitative PCR machine (Applied Biosystems™ One Step Plus qPCR) with the following program: one cycle of 50 °C for 2 minutes, one cycle of 95 °C for 10 minutes, 40 cycles of 95 °C for 15 seconds and 60 °C for 60 seconds.

rAAV transduction

Aliquots of previously titered viruses were thawed on ice and diluted in TFB2 to achieve the predetermined dose of $1.5x10^{11}$ GC in a 100 µL volume. Inbred 3- to 4-week old C57BL/6 (Jackson Laboratories) female mice, in groups of five, each was given a single 100 µL intramuscular (i.m.) injection into the cranial thigh muscle with a 29G needle. After vector administration, blood was collected from the tail weekly starting from week 3. Tubes were stored at 4 °C for 1 hour, then was spun for 10 minutes at 5,000 RPM to separate sera. Sera was collected and stored at −20 °C.

Inhibitor in vivo *properties characterization*

Mouse sera was diluted 1:5,000 with sterile blocking buffer (1% BSA in PBS and 0.1% TWEEN 20) as starting dilution for ELISA. For quantification of human IgG expression level: 100 µL diluted goat anti-human IgG-Fc antibody (Bethyl) was added in each well of the plate and incubate overnight at 4 °C. On the next day, 200 µL of blocking buffer was added to each well and incubated for 1 hour. Serum samples were serially diluted in blocking buffer starting from 1:5,000 on a clean 96-well plate. 100 µL of each sample dilution was added to the ELISA plate and incubated for 1 hour at room temperature. Plate was washed with wash buffer (1×PBS and 0.1% TWEEN 20) and incubated with 100 µL per well blocking-buffer-diluted HRP-conjugated goat anti-human kappa light chain antibody (1:10,000; Bethyl) for 1 hour at room temperature. Plate was washed again for four times, then 100 µL of TMB Super Sensitive 1-Component HRP Microwell Substrate was added into each well. The plate was incubated in the dark for 2 minutes at room temperature, followed by neutralization with 100 µL Stop Solution for TMB Substrates. Plate was read

at a wavelength of 650 nm then deduced by 450 nm signal using a microplate reader. A standard curve was generated based on the reading of Human Reference Serum (Bethyl), and OD data of the samples were interpolated using the standard curve to calculate the human IgG concentration in mice serum.

Immunofluorescent assay: blood smears were made from donor mice that were injected with *P. yoelii* parasites. Fixative solution (2.5% PFA, 0.1% GA, 3% sucrose) was added to the slide and incubated for 10 minutes, then aspirated with vacuum and the slide was washed with 1× PBS for 3 times. Next, blocking buffer (1× PBS, 2% BSA, 0.1% Triton X-100) was added on the slide and incubated for 1 hour at room temperature. Serum diluted 1:100 in blocking buffer was added to the slide, then gently covered with a coverslip (to avoid the coverslip contacting the smears). The slides were incubated at 4 °C overnight, then were washed with wash buffer (1× PBS and 0.1% Triton) for 5 times the next day. Secondary antibody (488 goat anti-human antibody) 1:200 diluted was added to the slide and kept in dark for 2 hours, then washed with wash buffer. Finally, 5 μL of ProLong™ Gold Antifade Mountant mounting solution was added and mounted with coverslips. Antibody to *Py*AMA1 (1:1,000 dilution) was added to confirm co-localization with *Py*-RON2L-Ig. Anti-rabbit Alexa Fluor® 633 was used on secondary antibody.

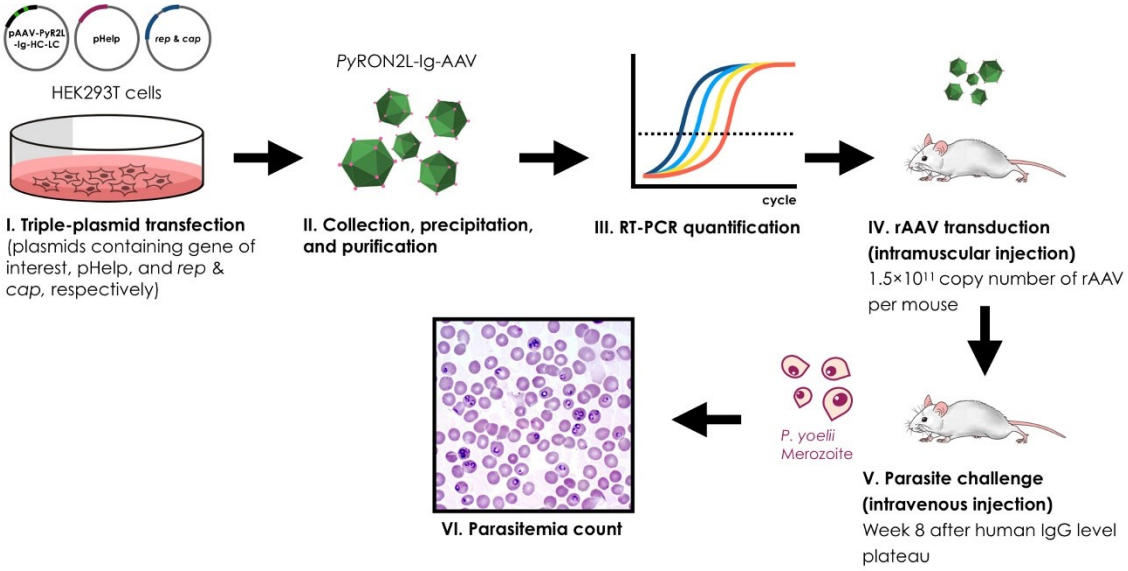

Figure 7. *In vivo* experiments overview. (**I**) Tissue culture is transfected with three plasmids: pAAV with gene of interest, pHelp, and *rep* and *cap* plasmid. (**II**) rAAV particles were precipitated and purified from the culture supernatant, followed by (**III**) RT-PCR quantification. (**IV**) Total 1.5×10^{11} GC of rAAV per mice is injected in the leg muscle, and *in vivo* expression level of the inhibitor is followed by weekly bleeding of the animal and human IgG quantification in the mouse sera by ELISA. (**V**) Once the inhibitor level starts to plateau starting from week 8, the mice are challenged with *P. yoelii* blood-stage parasites. (**VI**) Lastly, protection effect of the inhibitor is monitored by a daily bleeding of the animal and comparing the parasitemia of the blood smears made from experimental and control groups.

Results

Optimization of transfection

BioT is a lipid-based reagent designed and formulated with proprietary technology for transfecting DNA, siRNA and anti-sense oligonucleotides into a variety of eukaryotic cell lines, insect cells, and cells of primary culture and suspension culture[83]. BioT is what originally used in the Baltimore lab protocol for triple-plasmid transfection to produce recombinant viruses, yielding high copy number of recombinant viruses. However, for the purpose of producing proteins, previous experience with BioT resulted in low expression level. Hence, optimization of this process is required to obtain a higher transfection efficiency.

jetPRIME® is a novel powerful transfection reagent based on a polymer formulation manufactured at Polyplus-transfection®, and it only requires low amounts of nucleic acid per transfection, hence resulting in very low cytotoxicity. We compared transfection efficiency of green fluorescent protein (GFP) after transfecting HEK293T cells using the same amount (2 μg) of plasmid containing GFP with either BioT or jetPRIME. GFP expression was monitored using a fluorescent microscope (**Figure 8A & 8B**). Transfection with jetPRIME resulted in superior transfection efficiency as observed by the higher number of cells expressing GFP on the plate using jetPRIME with similar cell confluency as the plate using BioT (**Figure 8C & 8D**). Henceforth jetPRIME system was used for subsequent HEK293T cell transfections, including both *Pf*RON2L-Ig and recombinant AAV.

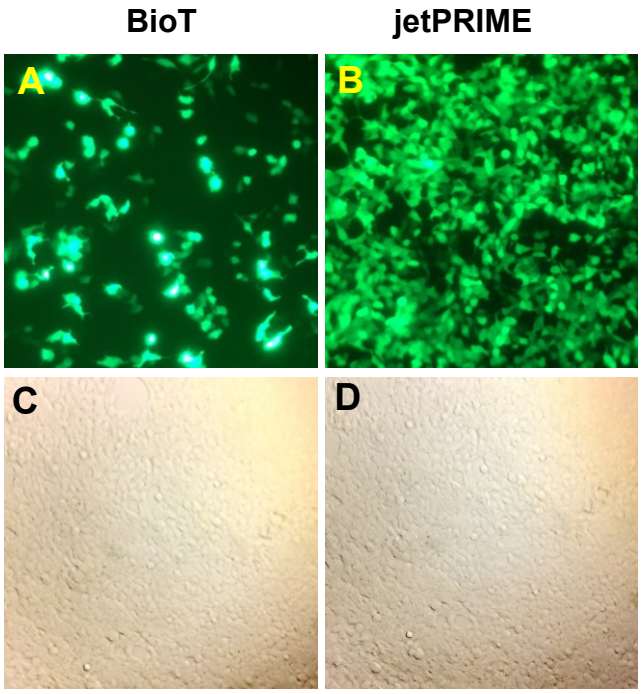

Figure 8. Transfection reagent optimization. GFP expression level in cells transfected with BioT (**A**) or jetPRIME (**B**) on 293T cell plates with similar cell confluency observed under bright field (**C** & **D**).

Inhibitor binds to its natural parasite ligand AMA1

ELISA data showed that in the cell culture supernatant, both heavy and light chain of the RON2L fusion protein were produced at high level. Importantly, these fusion proteins were able to bind to AMA1 individually (**Figure 9A**). Next, we examined the optimal HC:LC ratio for transfection to produce maximum RON2L-Ig quantity. Four different ratios were tested, while no significant difference in total Ig between them was observed, 1:1 ratio appears to have higher yield and stronger AMA1 binding activity (**Figure 9B**). Next, we tested the duration of recombinant RON2L-Ig protein expressed in the transfected 293T cells. To do this, we collected culture supernatant at different day following transfection and measured total Ig and its AMA1 binding activity. Inhibitor was produced at consistently high levels in 293T cell culture over the 2 weeks tested (**Figure 9C**).

In addition to inhibitor's ability to bind 3D7 AMA1, we also showed its specificity to bind AMA1 variants of different strains of *P. falciparum* parasites. The inhibitor showed similar binding affinity to both *Pf* 3D7 and *Pf*FVO AMA1, indicating that the recombinant RON2L-Ig indeed has cross-strain specificity (**Figure 9D**).

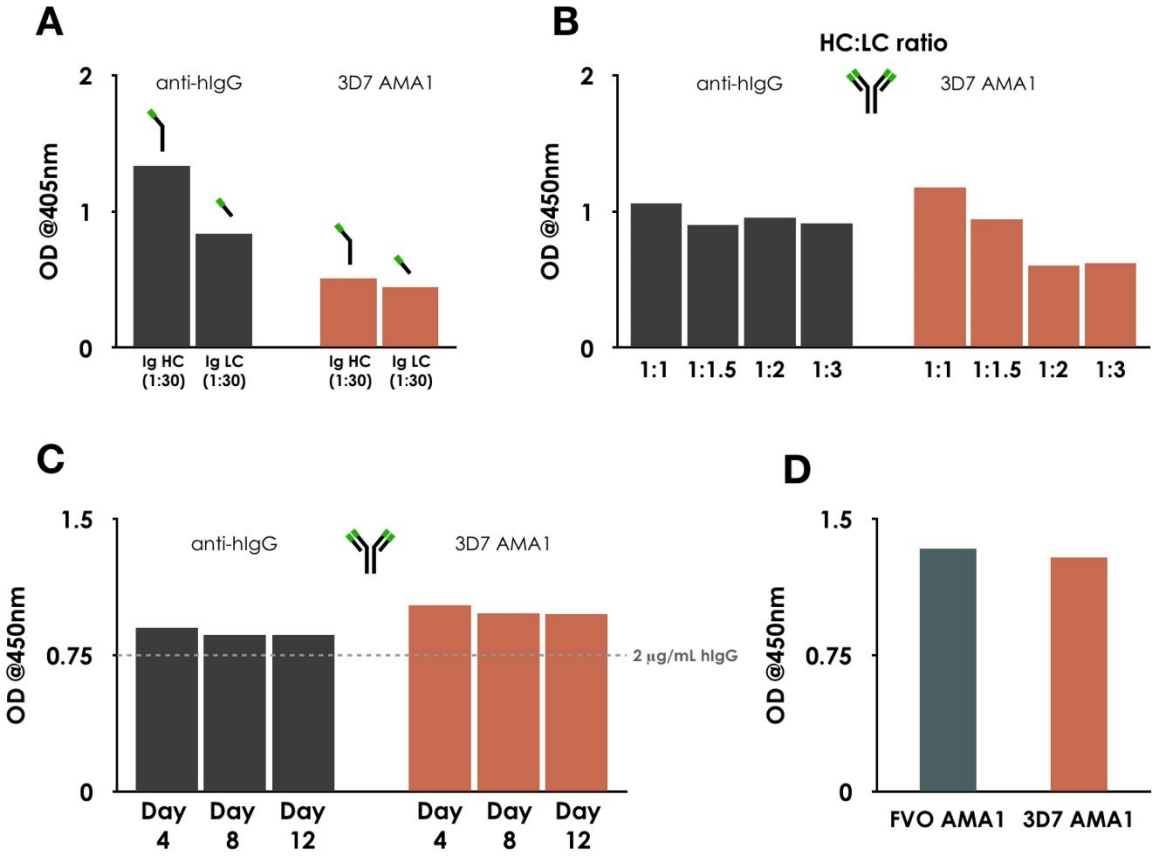

Figure 9. Characterization of *Pf*RON2L-Ig by ELISA. (A) HC and LC expression in 293T cells (anti-hIgG) and their binding activity to AMA1 (schematic representation of HC and LC is shown on the top of each column), **(B)** testing different plasmid ratios of HC:LC plasmids for transfection for optimal inhibitor expression (anti-hIgG) and its binding activity (3D7 AMA1), (**C**) stable *Pf*RON2L-Ig expression (anti-hIgG) in 293T cells over two weeks, with reference line showing the signal level of 2 µg/mL human IgG, and (**D**) *Pf*RON2L-Ig showing similar binding activity to recombinant AMA1 of *P. falciparum* 3D7 and FVO.

Optimization of inhibitor purification methods

Next, in order to obtain a relatively small volume of supernatant for purification, we tested two Ig precipitation methods using ammonium sulfate and sodium sulfate. We found that inhibitor precipitated using $(NH_4)_2SO_4$ demonstrated higher level of human IgG concentration and stronger binding activity against AMA1 in general. In addition, we detected less inhibitor remained in the supernatant after $(NH_4)_2SO_4$ precipitation (**Figure 10A & 10B**). Next, we evaluated the inhibitor's binding activity against 3D7 AMA1 under varying storage conditions by ELISA. Here we focused on analyzing how different storage buffers (1× PBS, DMEM, and incomplete RPMI) and inhibitor's concentration level (before and after dialysis) would affect its bio-activity after two weeks of storage at 4 °C. Aliquot of each sample stored at −80 °C for the same period of time was used as control. Remarkably, our data suggested that $(NH_4)_2SO_4$ precipitated inhibitor stored in incomplete RPMI had a well preserved bio-activity, in contrast to different degrees of activity loss observed in all other conditions (**Figure 11A-D**). We also showed that higher concentration did not have detectable negative effect on protein's activity (**Figure 11E**).

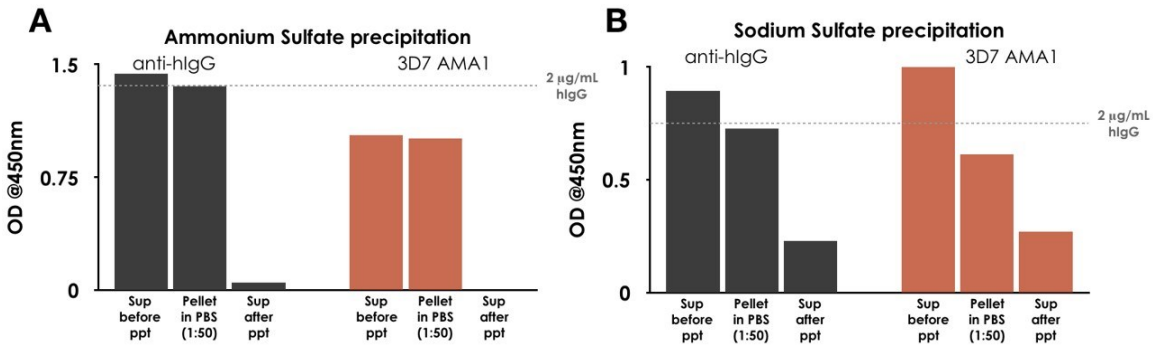

Figure 10. Protein precipitation using two different methods. Inhibitor concentration (anti-hIgG) and binding activity (3D7 AMA1) evaluation after **(A)** $(NH_4)_2SO_4$ and **(B)** Na_2SO_4 precipitation by ELISA.

Therefore, based on these evidences, we chose to use ammonium sulfate precipitation method for subsequent experiments, and the purified inhibitor protein was stored in incomplete RPMI at 4 °C.

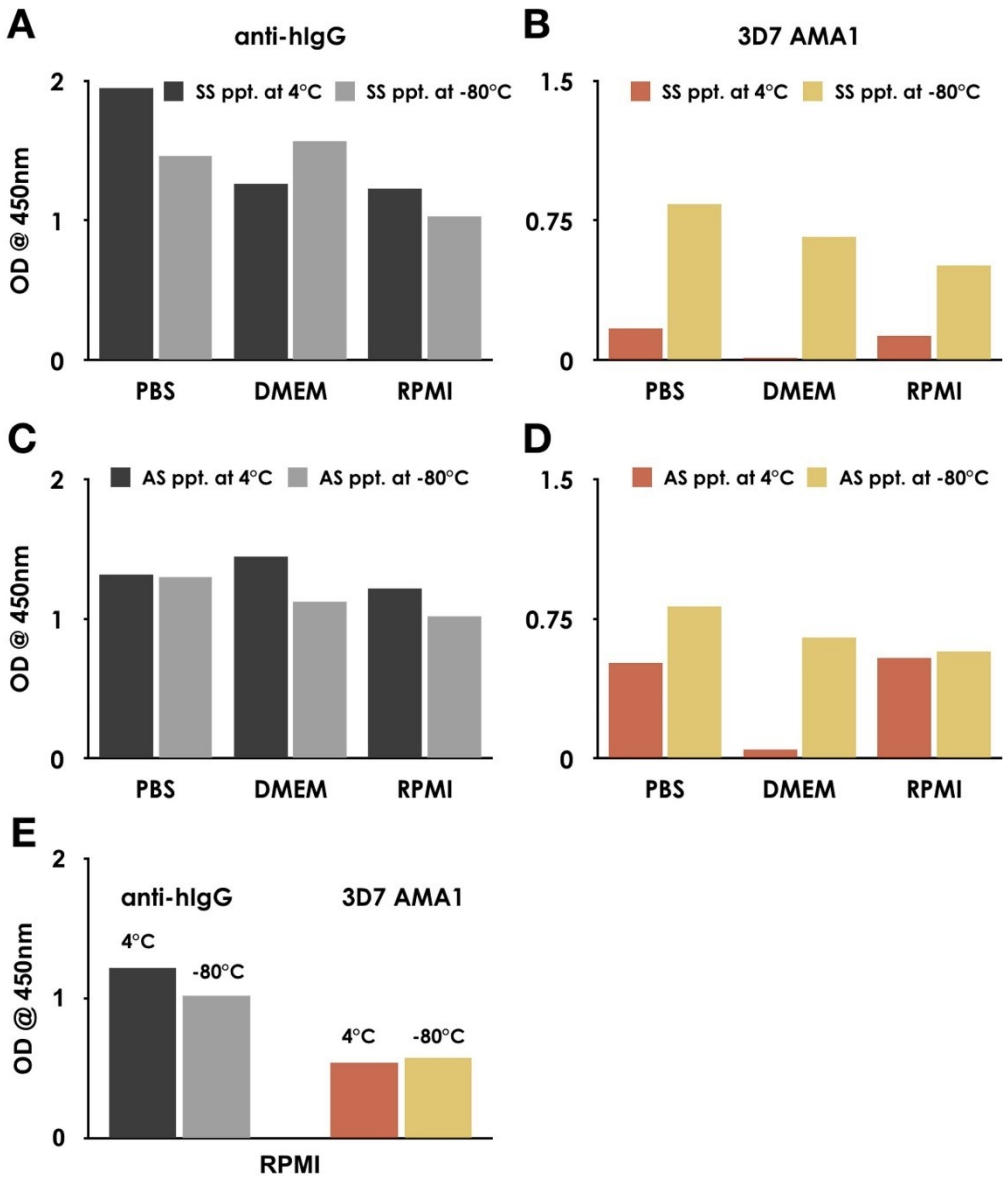

Figure 11. Stability evaluation of *Pf*RON2L-Ig by ELISA. After storing at 4 °C for two weeks, protein concentration was quantified (**A&C**, anti-hIgG) and its binding activity against 3D7 AMA1 was evaluated (**B&D**, 3D7 AMA1) by ELISA. (**E**). $(NH_4)_2SO_4$ precipitated inhibitor stored in incomplete RPMI at 4 °C showed no detectable change in activity after two weeks.

To purify RON2L-Ig, we used Protein G agarose column due to its ability to bind the Fc region of the immunoglobulin molecules. The $(NH_4)_2SO_4$ precipitated pellets from the cell culture supernatant was dissolved in small volume of 1× PBS and allowed to flow through the column as described in the Methods section. After Protein G column purification, the purified RON2L-Ig sample was loaded on an SDS-PAGE protein gel. Coomassie Blue stained protein gel showed that comparing to the supernatant before purification, a concentrated band appeared at approximately 150 kDa (**Figure 12A**), suggesting the inhibitor with a human IgG backbone successfully isolated from the supernatant. This was confirmed by western blot using an anti-human IgG antibody (**Figure 12B**). IFA images showed an overlap signal between the AMA1 (labeled with anti-AMA1 antibody) and inhibitor *Pf*RON2L-Ig (labeled with anti-human antibody), confirming that our inhibitor is able to bind natural parasite as designed (**Figure 12C**).

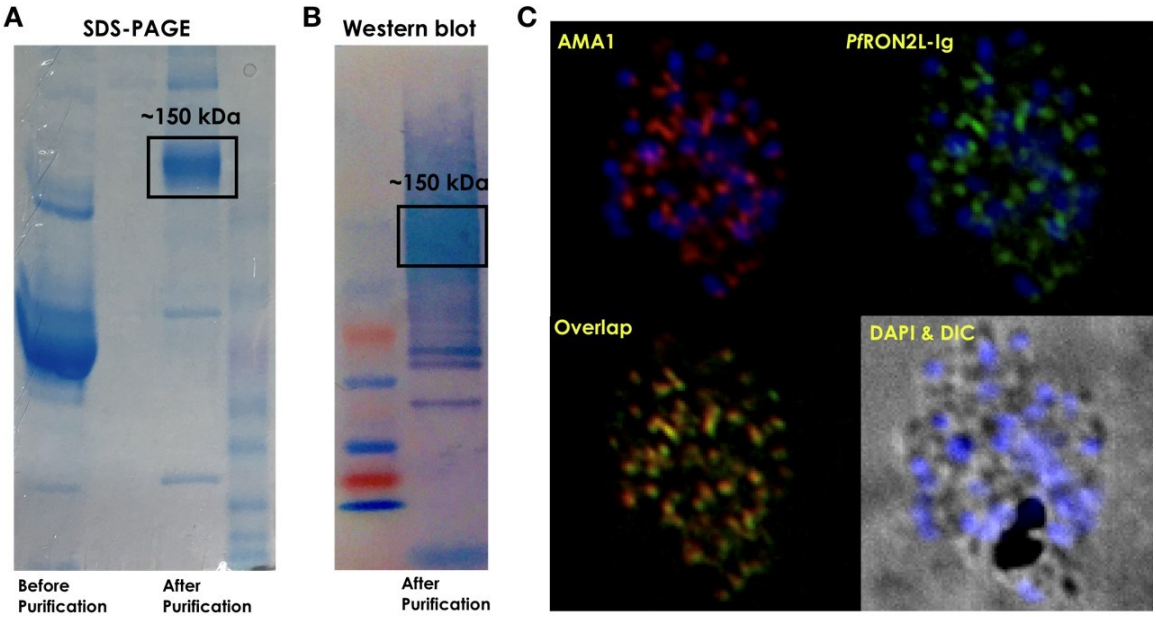

Figure 12. Purified *Pf*RON2L-Ig characterization. (A) Coomassie stained SDS-PAGE gel and (**B**) western blot of purified RON2L-Ig showing a concentrated band at approximately 150kDa. (**C**) IFA of *P. falciparum* showing co-localization between RON2L-Ig (Green signal) and anti-AMA1 Ab (Red signal).

Inhibitor effectively neutralizes parasite invasion in vitro

After demonstrating that the inhibitor does bind to natural AMA1 on the parasite surface, our next step is to confirm that, as hypothesized, the inhibitor can efficiently block the parasite invasion by competitively bind to AMA1 ligands on the parasite surface. To do this, parasites were first synchronized to late schizont stage, then GIA was performed by adding purified inhibitor *Pf*RON2L-Ig to *P. falciparum* parasite culture. After 48 hours, the samples were stained with MitoTracker and SYBR Green, and flow cytometry was used to measure cell fluorescence. Viable parasites were labeled with MitoTracker dyes, which permanently bound to mitochondria of the cells, whereas SYBR Green signal indicated the parasite-infected RBCs. Parasitemia was determined by the percentage of the cluster which is positive for both SYBR Green and MitoTracker.

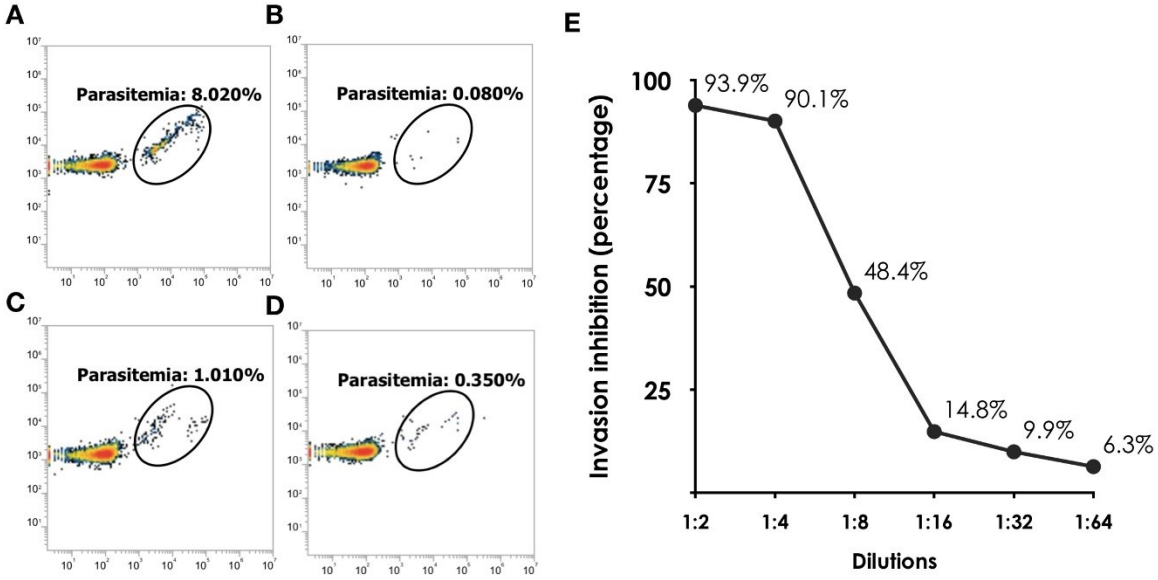

Figure 13. Growth inhibition assay for 48 hours. Parasitemia of (**A**) no-drug control parasite culture, (**B**) parasite culture added with inhibitor *Pf*RON2L-Ig (final concentration 300 μg/mL), (**C**) parasite culture added with EGTA (final concentration 4 mM), and (**D**) parasite culture added with E64D (final concentration 50 μM). (**E**) Dose-dependent inhibitory effect of *Pf*RON2L-Ig in 3D7 *P. falciparum* cultures.

Clusters with distinct SYBR Green signal strength represent various stages (e.g. ring stage, schizont stage) of the parasites inside infected RBCs (**Figure 13A**). The original concentration of the protein G column purified inhibitor quantified by ELISA was approximately 600 μg/mL (making the first dilution 300 μg/mL) and resulted in a 94% of inhibition effect (**Figure 13B**). The positive controls where final concentration of 4 mM EGTA or 50 μM E64D in the parasite culture and showed 90% and 95.6% of inhibition effect respectively (**Figure 13C & 13D**). Dose-dependent inhibitory effect was observed for serial diluted inhibitor (**Figure 13E**).

rAAV transduction induces in vivo *expression of the inhibitor*

Inhibitor level in the serum continued to increase starting from week 0 after recombinant AAV transduction and finally plateaued at 700-800 μg/mL starting from week 3 and week 4 for 2A10 and RON2L-Ig transduced mice respectively (**Figure 14A**). This level of expression was compatible to the results from previous studies[68,71]. As discussed previously, the inhibitor is a foreign peptide RON2L fused to a human Ig backbone, therefore we also tested if either part of the fused protein induced an immune response in these mice. ELISA data of mice serum on plates coated with human IgG antibody and RON2L peptides showed only a very low level of anti-human Ig antibody in these animals (**Figure 14B**). Importantly, the anti-RON2L antibody in the mice serum was absent or minimal (**Figure 14C**), suggesting that the engineered inhibitor showed little immunogenicity to the rAAV transduced mice.

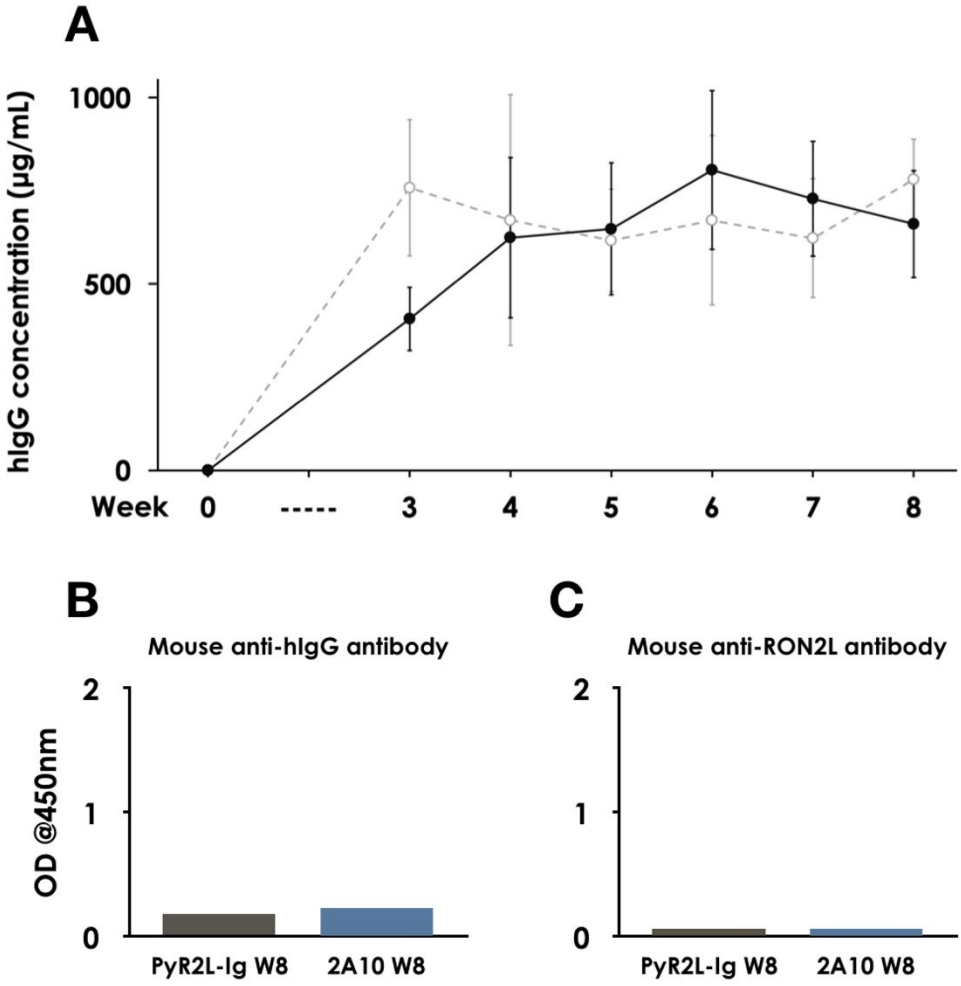

Figure 14. *In vivo* expressed inhibitor *Py*RON2L-Ig characterization by ELSIA. (**A**) Human IgG level in mouse sera after recombinant viral vector transduction followed for 8 weeks. (**B**) Anti-human IgG antibody and (**C**) anti-RON2L antibody level in week 8 sera samples.

Discussion

In 2016, 21 countries were identified by WHO as having the most potential to eliminate malaria by 2020, these include Mexico, Belize, El Salvador, Costa Rica, Ecuador, Suriname, Paraguay, Cabo Verde, Botswana, Algeria, South Africa, Comoros, Saudi Arabia, Iran, Nepal, Bhutan, China, Malaysia, Timor-Leste, and South Korea[84]. To date Paraguay is the only country that has been certified to be malaria-free by WHO, and while most of the 21 countries are on track to malaria elimination, there are still a few countries have concerning high yearly indigenous cases. For example, South Africa has close to 20,000 indigenous cases in 2017 alone, which is a dramatic increase comparing to that of 2016[2].

Previously, antibodies that target circumsporozoite proteins (CSP), such as monoclonal antibody 2A10[85,86], more recently identified CIS43[87], and two monoclonal antibodies mAbs 311 and 317[88], are the main focus of research for rational vaccine design or passive immunization. These mAbs mainly target a central region consisting predominantly of NANP repeats in the N-terminal domain of the *Pf* CSP, which is essential for *Plasmodium* life cycle and parasite development in the mosquito vector as well as in the mammalian host[89–91]. NANP is found to be conserved among *P. falciparum* isolated from diverse geographical locations[86], rendering it a potentially ideal target for *P. falciparum* immunization. B-cell response elicited by CSP results in production of antibodies that target mainly the central region of NANP repeats, protecting animal models from malaria infection[92,93]. However, clinical trials of RTS,S vaccine designed based on *Pf*CSP showed minimal and short-term protection effect in the absence of repeated immunization[10,94,95], possibly due to the lack of efficient formation of protective B cell memory[96,97].

The path to achieving the final goal of GTS to have at least 35 countries eliminate malaria before 2030 seems full of challenges, especially with the recent emergence of multi-drug resistant parasite strains. The current situation warrants us to seek alternative non-traditional solutions beyond current scope. Inspired and encouraged by the report published in 2015, in which the inhibitor eCD4-Ig delivered by viral vector in rhesus macaques and showed great protection effect against SHIV infection. This artificially designed inhibitor binds avidly and cooperatively to the HIV-1 envelope glycoprotein (Env) and is shown to be even more potent than the best broadly neutralizing antibody (bNAbs)[72]. In this study, preliminary data of a novel inhibitor *Pf*RON2L-Ig with a human immunoglobulin backbone has shown promising inhibitory effect on *Plasmodium falciparum* invasion process. We showed that the inhibitor can be produced by mammalian cells as correctly folded, intact fusion protein, and it can bind to multiple strains of AMA1 molecules. IFA data showed that the inhibitor can bind to the natural AMA1 molecule on the surface of the parasite, and GIA data showed that it efficiently blocks the parasite invasion process *in vivo.* Next, we used an adeno-associated viral vector to deliver the gene of the inhibitor in our *in vivo* mice model and we detected high expression level in their bloodstream (~700 μg/mL in average). In theory, in addition to the expected direct blocking of invasion by parasites, it is possible that our inhibitor *Pf*RON2L-Ig could also come to effect by (1) the neutralization of parasites by agglutination, (2) the initiation of the complement cascade resulting in further opsonization and lysis, and (3) the recruitment of neutrophilic granulocytes and monocytes. However, analysis of these immune responses is beyond the scope of this study thus will not be further discussed here.

Despite of the strong inhibitory effect observed in GIA experiments, activity loss of the purified inhibitor *Pf*RON2L-Ig was observed after two weeks of storage at 4 °C (**Figure 11**), likely due to protein's instability. The close proximity between the RON2L peptide on the heavy and light chains might lead to the formation of cross-disulfide bond between the RON2L peptides on the heavy and the light chain thus the disruption of the tertiary structure. A potential solution to the problem could be instead of a tetravalent inhibitor (i.e. all four variable regions on a single immunoglobulin are replaced with RON2L), a divalent inhibitor with only the heavy chains replaced by RON2L should be tested. This could presumably avoid close contact between two chains and consequently the potential cross-disulfide bond formation. Another possibility is that the instability of the fusion protein was caused by the flexible linker sequence attached between RON2L and Ig. It was reported that the secondary structure, the hydrophobicity, the amino acid residues, and the length of the linker may play important role in the yield and the bioactivity of fusion proteins[98]. For example, in the case of a bifunctional enzyme that is the fusion protein of β-glucanase and xylanase, compared to flexible linkers, the insertion of longer helical linkers $(EAAAK)_n$ (n = 1-3) appeared to be more efficient in increasing the thermal stability[99]. It is likely that the rigid structure of the α-helical linker might provide space for different domains of the fusion protein to fold and function independently. Another possibility is to increase the length of linker to provide better stability. The linker used in this study has only a single repeat of Gly-Gly-Ser-Gly between RON2L peptide and the constant region of Ig, therefore it is possible that by adjusting the length and the secondary structure of the linker, the thermal stability could be improved.

Our next goal is to evaluate inhibitor's protection efficiency in the process of sporozoite (the form injected by infected mosquitoes) entry into hepatocytes. IFA will be performed to verify it binding to the surface of sporozoites, which will be obtained by dissecting infected mosquitoes. Gliding motility assay will also be performed to assess the effect of inhibitor *Py*RON2L-Ig on parasite motility. Next, mice will first be injected intramuscularly with the optimal number of AAV-*Py*RON2L-Ig to have the inhibitor expressed at high level as described above, then 2 to 4 weeks after transduction will be challenged by intravenous injection of 1,000 sporozoites isolated from the salivary gland of infected mosquitoes. Mice will be sacrificed 36 hours after challenge, before the release of hepatic merozoites that infect RBC, and parasite load in the liver will be measured by qPCR using primers specific for *Plasmodium* 18S rRNA. Completion of this arm of the study will confirm that in addition to prevention of blood stage infection, which leads to the clinical symptoms, the inhibitor is also able to prevent the initiation of infection and *in vivo* transmission from the very start—sporozoite invasion into hepatocytes.

In spite of the potential advantages described above, preexisting immunity against viral capsid, which can lead to low transduction efficiency of rAAV, has been one of the biggest concerns in the use of the VIP technology in human trials[100,101]. For example a study detected prevalence of IgG against most of the commonly used AAV serotypes in human: anti-AAV1 and -AAV2 total IgG determined by enzyme-linked immunosorbent assay showed 67% and 72%, higher than those of anti-AAV5 (40%), anti-AAV6 (46%), anti-AAV8 (38%), and anti-AAV9 (47%)[102]. In addition, studies also identified CD4+ and CD8+ T cell epitopes for AAV2[103–105] and AAV8[106]. New approaches such as engineering

viral capsids by directed evolution could lead to discovery of low immunogenic viral vectors thus an improved transduction efficiency[107]. It is important to evaluate the anti-AAV capsid antibody level in the animal model during the future experiments. In addition to the immunity against viral vector, there is also the potential immune response against the artificially designed inhibitor (i.e. elicitation of anti-inhibitor antibody). For example, a recent study showed that the artificial inhibitor eCD4-Ig designed for HIV induced strong host immune response due to the immunogenicity of IgG1-Fc region of the inhibitor; while in contrast, eCD4-Ig bearing a rhesus IgG2-Fc domain showed reduced immunogenicity and correlated with stronger protection in rhesus macaques[108]. Although our preliminary data showed no detection of anti-inhibitor antibody in the mouse sera at week 8 (**Figure 14B & 14C**), it does not guarantee a similar level of immune response would be seen in NHP or human. Further experiments are required to examine the inhibitor's immunogenicity.

In conclusion, our study has tested the engineered *P. falciparum* self-targeting entry inhibitor RON2L-Ig both *in vitro* and *in vivo* to evaluate (1) its inhibitory effect for blocking parasite invasion and (2) its expression level in animal sera when delivered by a viral vector. Our preliminary data showed that the inhibitor can efficiently inhibit parasite invasion *in vitro* presumably by competitively binding to AMA1 molecule on the parasite surface, and it can also be expressed at high level *in vivo* in a mouse model. However, further studies are needed to optimize its stability and confirm both its inhibitory effect *in vivo*. This study aims to eventually provide a novel solution to the malaria infection by using viral vector to deliver an inhibitor that self-targets a key step used by malaria parasites to enter host cells.

Reference

1. World Health Organization & World Health Organization. Global Malaria Programme. *Global technical strategy for malaria, 2016-2030*. *WHO Geneva* (2015).

2. World Health Organisation. *World Malaria Report*. *World Malaria Report* (2018). doi:ISBN 978 92 4 156483 0

3. Hemingway, J., Field, L. & Vontas, J. An overview of insecticide resistance. *Science* (2002). doi:10.1126/science.1078052

4. Liu, N. Insecticide Resistance in Mosquitoes: Impact, Mechanisms, and Research Directions. *Annu. Rev. Entomol.* (2015). doi:10.1146/annurev-ento-010814-020828

5. Takala-Harrison, S. *et al.* Independent emergence of artemisinin resistance mutations among Plasmodium falciparum in Southeast Asia. *J. Infect. Dis.* (2015). doi:10.1093/infdis/jiu491

6. Miotto, O. *et al.* Genetic architecture of artemisinin-resistant Plasmodium falciparum. *Nat. Genet.* (2015). doi:10.1038/ng.3189

7. Sheiner, L., Vaidya, A. B. & McFadden, G. I. The metabolic roles of the endosymbiotic organelles of Toxoplasma and Plasmodium spp. *Current Opinion in Microbiology* (2013). doi:10.1016/j.mib.2013.07.003

8. Phillips, M. A. *et al.* Malaria. *Nat. Rev. Dis. Prim.* **3**, 17050 (2017).

9. Sidjanski, S. & Vanderberg, J. P. Delayed migration of Plasmodium sporozoites from the mosquito bite site to the blood. *Am. J. Trop. Med. Hyg.* (1997). doi:10.4269/ajtmh.1997.57.426

10. Crompton, P. D. *et al.* Malaria Immunity in Man and Mosquito: Insights into Unsolved Mysteries of a Deadly Infectious Disease. *Annu. Rev. Immunol.* (2014). doi:10.1146/annurev-immunol-032713-120220

11. Barillas-Mury, C. & Kumar, S. Plasmodium-mosquito interactions: A tale of dangerous liaisons. *Cellular Microbiology* (2005). doi:10.1111/j.1462-

5822.2005.00615.x

12. Sim, B. K. L. *et al.* Primary structure of the 175K Plasmodium falciparum erythrocyte binding antigen and identification of a peptide which elicits antibodies that inhibit malaria merozoite invasion. *J. Cell Biol.* (1990). doi:10.1083/jcb.111.5.1877

13. Orlandi, P. A., Klotz, F. W. & Haynes, J. D. A malaria invasion receptor, the 175-kilodalton erythrocyte binding antigen of Plasmodium falciparum recognizes the terminal Neu5Ac(α2-3)Gal- sequences of glycophorin A. *J. Cell Biol.* (1992). doi:10.1083/jcb.116.4.901

14. Duraisingh, M. T. *et al.* Phenotypic variation of Plasmodium falciparum merozoite proteins directs receptor targeting for invasion of human erythrocytes. *EMBO J.* (2003). doi:10.1093/emboj/cdg096

15. Triglia, T. *et al.* Identification of proteins from Plasmodium falciparum that are homologous to reticulocyte binding proteins in Plasmodium vivax. *Infect. Immun.* (2001). doi:10.1128/IAI.69.2.1084-1092.2001

16. Rayner, J. C., Galinski, M. R., Ingravallo, P. & Barnwell, J. W. Two Plasmodium falciparum genes express merozoite proteins that are related to Plasmodium vivax and Plasmodium yoelii adhesive proteins involved in host cell selection and invasion. *Proc. Natl. Acad. Sci.* (2002). doi:10.1073/pnas.160469097

17. Singh, S., Alam, M. M., Pal-Bhowmick, I., Brzostowski, J. A. & Chitnis, C. E. Distinct external signals trigger sequential release of apical organelles during erythrocyte invasion by malaria parasites. *PLoS Pathog.* (2010). doi:10.1371/journal.ppat.1000746

18. Dvorak, J. A., Miller, L. H., Whitehouse, W. C. & Shiroishi, T. Invasion of erythrocytes by malaria merozoites. *Science (80-.).* (1975). doi:10.1126/science.803712

19. Aikawa, M., Miller, L. H., Johnson, J. & Rabbege, J. Erythrocyte entry by malarial parasites. A moving junction between erythrocyte and parasite. *J. Cell Biol.* (1978). doi:10.1083/jcb.77.1.72

20. Miller, L. H. Interaction between cytochalasin B-treated malarial parasites and erythrocytes. Attachment and junction formation. *J. Exp. Med.* (2004). doi:10.1084/jem.149.1.172

21. Baum, J. *et al.* A conserved molecular motor drives cell invasion and gliding motility across malaria life cycle stages and other apicomplexan parasites. *J. Biol. Chem.* (2006). doi:10.1074/jbc.M509807200

22. Triglia, T. *et al.* Apical membrane antigen 1 plays a central role in erythrocyte invasion by Plasmodium species. *Mol. Microbiol.* (2000). doi:10.1046/j.1365-2958.2000.02175.x

23. Hehl, A. B. *et al.* Toxoplasma gondii homologue of plasmodium apical membrane antigen 1 is involved in invasion of host cells. *Infect. Immun.* (2000). doi:10.1128/IAI.68.12.7078-7086.2000

24. Mital, J. Conditional Expression of Toxoplasma gondii Apical Membrane Antigen-1 (TgAMA1) Demonstrates That TgAMA1 Plays a Critical Role in Host Cell Invasion. *Mol. Biol. Cell* (2005). doi:10.1091/mbc.e05-04-0281

25. Donahue, C. G., Carruthers, V. B., Gilk, S. D. & Ward, G. E. The Toxoplasma homolog of Plasmodium apical membrane antigen-1 (AMA-1) is a microneme protein secreted in response to elevated intracellular calcium levels. *Mol. Biochem. Parasitol.* (2000). doi:10.1016/S0166-6851(00)00289-9

26. Healer, J., Crawford, S., Ralph, S., McFadden, G. & Cowman, A. F. Independent translocation of two micronemal proteins in developing Plasmodium falciparum merozoites. *Infect. Immun.* (2002). doi:10.1128/IAI.70.10.5751-5758.2002

27. Narum, D. L. & Thomas, A. W. Differential localization of full-length and processed forms of PF83/AMA-1 an apical membrane antigen of Plasmodium falciparum merozoites. *Mol. Biochem. Parasitol.* (1994). doi:10.1016/0166-6851(94)90096-5

28. Howell, S. A., Withers-Martinez, C., Kocken, C. H. M., Thomas, A. W. & Blackman, M. J. Proteolytic Processing and Primary Structure of Plasmodium falciparum Apical Membrane Antigen-1. *J. Biol. Chem.* (2001).

doi:10.1074/jbc.M103076200

29. Chesne-Seck, M. L. *et al.* Structural comparison of apical membrane antigen 1 orthologues and paralogues in apicomplexan parasites. *Mol. Biochem. Parasitol.* (2005). doi:10.1016/j.molbiopara.2005.07.007

30. Alexander, D. L., Mital, J., Ward, G. E., Bradley, P. & Boothroyd, J. C. Identification of the moving junction complex of Toxoplasma gondii: A collaboration between distinct secretory organelles. *PLoS Pathog.* (2005). doi:10.1371/journal.ppat.0010017

31. Alexander, D. L., Arastu-Kapur, S., Dubremetz, J.-F. & Boothroyd, J. C. Plasmodium falciparum AMA1 Binds a Rhoptry Neck Protein Homologous to TgRON4, a Component of the Moving Junction in Toxoplasma gondii . *Eukaryot. Cell* (2006). doi:10.1128/ec.00040-06

32. Srinivasan, P. *et al.* Binding of Plasmodium merozoite proteins RON2 and AMA1 triggers commitment to invasion . *Proc. Natl. Acad. Sci.* (2011). doi:10.1073/pnas.1110303108

33. Tyler, J. S. & Boothroyd, J. C. The C-terminus of Toxoplasma RON2 provides the crucial link between AMA1 and the host-associated invasion complex. *PLoS Pathog.* (2011). doi:10.1371/journal.ppat.1001282

34. Lamarque, M. *et al.* The RON2-AMA1 interaction is a critical step in moving junction-dependent invasion by apicomplexan parasites. *PLoS Pathog.* (2011). doi:10.1371/journal.ppat.1001276

35. Bai, T. *et al.* Structure of AMA1 from Plasmodium falciparum reveals a clustering of polymorphisms that surround a conserved hydrophobic pocket. *Proc. Natl. Acad. Sci.* (2005). doi:10.1073/pnas.0501808102

36. Coley, A. M. *et al.* Structure of the malaria antigen AMA1 in complex with a growth-inhibitory antibody. *PLoS Pathog.* (2007). doi:10.1371/journal.ppat.0030138

37. Pizarro, J. C. *et al.* Crystal structure of the malaria vaccine candidate apical membrane antigen 1. *Science (80-.).* (2005). doi:10.1126/science.1107449

38. Tonkin, M. L. *et al.* Host cell invasion by apicomplexan parasites: insights from the co-structure of AMA1 with a RON2 peptide. *Science* **333**, 463–7 (2011).

39. Silvie, O. *et al.* A Role for Apical Membrane Antigen 1 during Invasion of Hepatocytes by Plasmodium falciparum Sporozoites. *J. Biol. Chem.* (2004). doi:10.1074/jbc.M311331200

40. Yang, A. S. P. *et al.* AMA1 and MAEBL are important for Plasmodium falciparum sporozoite infection of the liver. *Cell. Microbiol.* (2017). doi:10.1111/cmi.12745

41. Thomas, A. W., Waters, A. P. & Carr, D. Analysis of variation in PF83, an erythrocytic merozoite vaccine candidate antigen of Plasmodium falciparum. *Mol. Biochem. Parasitol.* (1990). doi:10.1016/0166-6851(90)90172-I

42. Takala, S. L. *et al.* Extreme polymorphism in a vaccine antigen and risk of clinical malaria: Implications for vaccine development. *Sci. Transl. Med.* (2009). doi:10.1126/scitranslmed.3000257

43. Coley, A. M. *et al.* The most polymorphic residue on Plasmodium falciparum apical membrane antigen 1 determines binding of an invasion-inhibitory antibody. *Infect. Immun.* (2006). doi:10.1128/IAI.74.5.2628-2636.2006

44. Ouattara, A. *et al.* Lack of allele-specific efficacy of a bivalent AMA1 malaria vaccine. *Malar. J.* (2010). doi:10.1186/1475-2875-9-175

45. Thera, M. A. *et al.* A Field Trial to Assess a Blood-Stage Malaria Vaccine. *N. Engl. J. Med.* (2011). doi:10.1056/nejmoa1008115

46. Srinivasan, P. *et al.* Immunization with a functional protein complex required for erythrocyte invasion protects against lethal malaria. *Proc. Natl. Acad. Sci.* (2014). doi:10.1073/pnas.1409928111

47. Srinivasan, P. *et al.* A malaria vaccine protects Aotus monkeys against virulent Plasmodium falciparum infection. *npj Vaccines* (2017). doi:10.1038/s41541-017-0015-7

48. Srinivasan, P. *et al.* Disrupting malaria parasite AMA1-RON2 interaction with a

small molecule prevents erythrocyte invasion. *Nat. Commun.* (2013). doi:10.1038/ncomms3261

49. Shi, J., Mcintosh, R. S. & Pleass, R. J. Antibody- and Fc-receptor-based therapeutics for malaria. *Clin. Sci.* (2005). doi:10.1042/cs20050136

50. Kennedy, M. C. *et al.* In vitro studies with recombinant Plasmodium falciparum apical membrane antigen 1 (AMA1): Production and activity of an AMA1 vaccine and generation of a multiallelic response. *Infect. Immun.* (2002). doi:10.1128/IAI.70.12.6948-6960.2002

51. Healer, J. *et al.* Allelic polymorphisms in apical membrane antigen-1 are responsible for evasion of antibody-mediated inhibition in Plasmodium falciparum. *Mol. Microbiol.* (2004). doi:10.1111/j.1365-2958.2003.03974.x

52. Bouharoun-Tayoun, H., Oeuvray, C., Lunel, F. & Druilhe, P. Mechanisms underlying the monocyte-mediated antibody-dependent killing of Plasmodium falciparum asexual blood stages. *J. Exp. Med.* (1995).

53. Jafarshad, A. *et al.* A Novel Antibody-Dependent Cellular Cytotoxicity Mechanism Involved in Defense against Malaria Requires Costimulation of Monocytes Fc RII and Fc RIII. *J. Immunol.* (2014). doi:10.4049/jimmunol.178.5.3099

54. Boyle, M. J. *et al.* Human antibodies fix complement to inhibit plasmodium falciparum invasion of erythrocytes andare associated with protection against malaria. *Immunity* (2015). doi:10.1016/j.immuni.2015.02.012

55. ATCHISON, R. W., CASTO, B. C. & HAMMON, W. M. ADENOVIRUS-ASSOCIATED DEFECTIVE VIRUS PARTICLES. *Science* (1965).

56. Buller, R. M., Janik, J. E., Sebring, E. D. & Rose, J. A. Herpes simplex virus types 1 and 2 completely help adenovirus-associated virus replication. *J. Virol.* (1981).

57. Smith, R. H. Adeno-associated virus integration: Virus versus vector. *Gene Therapy* (2008). doi:10.1038/gt.2008.55

58. Weitzman, M. D. & Linden, R. M. Adeno-associated virus biology. *Methods in*

Molecular Biology (2011). doi:10.1007/978-1-61779-370-7_1

59. Valdmanis, P. N., Lisowski, L. & Kay, M. A. rAAV-Mediated Tumorigenesis: Still Unresolved After an AAV Assault. *Mol. Ther.* (2012). doi:10.1038/mt.2012.220

60. Li, H. *et al.* Assessing the potential for AAV vector genotoxicity in a murine model. *Blood* (2011). doi:10.1182/blood-2010-08-302729

61. Nathwani, A. C. *et al.* Adenovirus-associated virus vector-mediated gene transfer in hemophilia B. *N. Engl. J. Med.* (2011). doi:10.1056/NEJMoa1108046

62. Jaski, B. E. *et al.* Calcium Upregulation by Percutaneous Administration of Gene Therapy in Cardiac Disease (CUPID Trial), a First-in-Human Phase 1/2 Clinical Trial. *J. Card. Fail.* (2009). doi:10.1016/j.cardfail.2009.01.013

63. LeWitt, P. A. *et al.* AAV2-GAD gene therapy for advanced Parkinson's disease: A double-blind, sham-surgery controlled, randomised trial. *Lancet Neurol.* (2011). doi:10.1016/S1474-4422(11)70039-4

64. Stroes, E. S. *et al.* Intramuscular Administration of AAV1-Lipoprotein Lipase S447X Lowers Triglycerides in Lipoprotein Lipase–Deficient Patients . *Arterioscler. Thromb. Vasc. Biol.* (2008). doi:10.1161/atvbaha.108.175620

65. Scott, L. J. Alipogene tiparvovec: A review of its use in adults with familial lipoprotein lipase deficiency. *Drugs* (2015). doi:10.1007/s40265-014-0339-9

66. Russell, S. *et al.* Efficacy and safety of voretigene neparvovec (AAV2-hRPE65v2) in patients with RPE65-mediated inherited retinal dystrophy: a randomised, controlled, open-label, phase 3 trial. *Lancet* (2017). doi:10.1016/S0140-6736(17)31868-8

67. Johnson, P. R. *et al.* Vector-mediated gene transfer engenders long-lived neutralizing activity and protection against SIV infection in monkeys. *Nat. Med.* (2009). doi:10.1038/nm.1967

68. Balazs, A. B. *et al.* Antibody-based protection against HIV infection by vectored immunoprophylaxis. *Nature* (2012). doi:10.1038/nature10660

69. Balazs, A. B., Bloom, J. D., Hong, C. M., Rao, D. S. & Baltimore, D. Broad protection against influenza infection by vectored immunoprophylaxis in mice. *Nat. Biotechnol.* (2013). doi:10.1038/nbt.2618

70. Balazs, A. B. *et al.* Vectored immunoprophylaxis protects humanized mice from mucosal HIV transmission. *Nat. Med.* (2014). doi:10.1038/nm.3471

71. Deal, C. *et al.* Vectored antibody gene delivery protects against Plasmodium falciparum sporozoite challenge in mice. *Proc. Natl. Acad. Sci.* (2014). doi:10.1073/pnas.1407362111

72. Gardner, M. R. *et al.* AAV-expressed eCD4-Ig provides durable protection from multiple SHIV challenges. *Nature* (2015). doi:10.1038/nature14264

73. Davis-Gardner, M. E., Gardner, M. R., Alfant, B. & Farzan, M. eCD4-Ig promotes ADCC activity of sera from HIV-1-infected patients. *PLoS Pathog.* (2017). doi:10.1371/journal.ppat.1006786

74. Fetzer, I. *et al.* eCD4-Ig Variants That More Potently Neutralize HIV-1. *J. Virol.* (2018). doi:10.1128/jvi.02011-17

75. Argos, P. An investigation of oligopeptides linking domains in protein tertiary structures and possible candidates for general gene fusion. *J. Mol. Biol.* (1990). doi:10.1016/0022-2836(90)90085-Z

76. George, R. A. & Heringa, J. An analysis of protein domain linkers: their classification and role in protein folding. *Protein Eng. Des. Sel.* (2003). doi:10.1093/protein/15.11.871

77. Kober, L., Zehe, C. & Bode, J. Optimized signal peptides for the development of high expressing CHO cell lines. *Biotechnol. Bioeng.* (2013). doi:10.1002/bit.24776

78. Polyplus-transfection® SA. jetPRIME® in vitro DNA & siRNA transfection reagent protocol. (2015). Available at: www.polyplus-transfection.com. (Accessed: 17th April 2019)

79. Aley, S. B. Knob-positive and knob-negative Plasmodium falciparum differ in expression of a strain-specific malarial antigen on the surface of infected

erythrocytes. *J. Exp. Med.* (2004). doi:10.1084/jem.160.5.1585

80. Xiao, X., Li, J. & Samulski, R. J. Production of high-titer recombinant adeno-associated virus vectors in the absence of helper adenovirus. *J. Virol.* (1998).

81. Matsushita, T. *et al.* Adeno-associated virus vectors can be efficiently produced without helper virus. *Gene Ther.* (1998). doi:10.1038/sj.gt.3300680

82. Graham, F. L., Smiley, J., Russell, W. C. & Nairn, R. Characteristics of a human cell line transformed by DNA from human adenovirus type 5. *J. Gen. Virol.* (1977). doi:10.1099/0022-1317-36-1-59

83. Bioland Scientific LLC. BioT Cell Transfection Manual. (2012). Available at: http://bioland-sci.com/PDF/BioT manual.pdf. (Accessed: 1st April 2019)

84. World Health Organization & Global Malaria Programme. *A Framework for Malaria Elimination*. *WHO Press, World Health Organization* (2017). doi:Licence: CC BY-NC-SA 3.0 IGO.

85. Nardin, E. H. Circumsporozoite proteins of human malaria parasites Plasmodium falciparum and Plasmodium vivax. *J. Exp. Med.* (2004). doi:10.1084/jem.156.1.20

86. Zavala, F., Hollingdale, M. R., Schwartz, A. L., Nussenzweig, R. S. & Nussenzweig, V. Immunoradiometric assay to measure the in vitro penetration of sporozoites of malaria parasites into hepatoma cells. *J. Immunol.* (1985).

87. Kisalu, N. K. *et al.* A human monoclonal antibody prevents malaria infection by targeting a new site of vulnerability on the parasite. *Nat. Med.* (2018). doi:10.1038/nm.4512

88. Oyen, D. *et al.* Structural basis for antibody recognition of the NANP repeats in Plasmodium falciparum circumsporozoite protein. *Proc. Natl. Acad. Sci. U. S. A.* (2017). doi:10.1073/pnas.1715812114

89. Cerami, C. *et al.* The basolateral domain of the hepatocyte plasma membrane bears receptors for the circumsporozoite protein of plasmodium falciparum sporozoites. *Cell* (1992). doi:10.1016/0092-8674(92)90251-7

90. Ménard, R. *et al.* Circumsporozoite protein is required for development of malaria

sporozoites in mosquitoes. *Nature* (1997). doi:10.1038/385336a0

91. Sidjanski, S. P., Vanderberg, J. P. & Sinnis, P. Anopheles stephensi salivary glands bear receptors for region I of the circumsporozoite protein of Plasmodium falciparum. *Mol. Biochem. Parasitol.* (1997). doi:10.1016/S0166-6851(97)00124-2

92. Sumitani, M. *et al.* Reduction of malaria transmission by transgenic mosquitoes expressing an antisporozoite antibody in their salivary glands. *Insect Mol. Biol.* (2013). doi:10.1111/j.1365-2583.2012.01168.x

93. Foquet, L. *et al.* Vaccine-induced monoclonal antibodies targeting circumsporozoite protein prevent Plasmodium falciparum infection. *J. Clin. Invest.* (2014). doi:10.1172/JCI70349

94. Moran, M. *et al. THE MALARIA PRODUCT PIPELINE: PLANNING FOR THE FUTURE*. (2007).

95. RTS,S Clinical Trials Partnership *et al.* A phase 3 trial of RTS,S/AS01 malaria vaccine in African infants. *N. Engl. J. Med.* (2012). doi:10.1056/NEJMoa1208394

96. Portugal, S., Pierce, S. K. & Crompton, P. D. Young Lives Lost as B Cells Falter: What We Are Learning About Antibody Responses in Malaria. *J. Immunol.* (2013). doi:10.4049/jimmunol.1203067

97. Struik, S. S. & Riley, E. M. Does malaria suffer from lack of memory? *Immunological Reviews* (2004). doi:10.1111/j.0105-2896.2004.00181.x

98. Chen, X., Zaro, J. L. & Shen, W.-C. Fusion protein linkers: property, design and functionality. *Adv. Drug Deliv. Rev.* (2013). doi:10.1016/j.addr.2012.09.039

99. Lu, P. & Feng, M. G. Bifunctional enhancement of a β-glucanase-xylanase fusion enzyme by optimization of peptide linkers. *Appl. Microbiol. Biotechnol.* (2008). doi:10.1007/s00253-008-1468-4

100. Kay, M. A. State-of-the-art gene-based therapies: The road ahead. *Nature Reviews Genetics* (2011). doi:10.1038/nrg2971

101. Mingozzi, F. & High, K. A. Immune responses to AAV vectors: Overcoming barriers to successful gene therapy. *Blood* (2013). doi:10.1182/blood-2013-01-

306647

102. Boutin, S. *et al.* Prevalence of Serum IgG and Neutralizing Factors Against Adeno-Associated Virus (AAV) Types 1, 2, 5, 6, 8, and 9 in the Healthy Population: Implications for Gene Therapy Using AAV Vectors. *Hum. Gene Ther.* (2010). doi:10.1089/hum.2009.182

103. Manno, C. S. *et al.* Successful transduction of liver in hemophilia by AAV-Factor IX and limitations imposed by the host immune response. *Nat. Med.* (2006). doi:10.1038/nm1358

104. Mingozzi, F. *et al.* CD8+ T-cell responses to adeno-associated virus capsid in humans. *Nat. Med.* (2007). doi:10.1038/nm1549

105. Madsen, D., Cantwell, E. R., O'Brien, T., Johnson, P. A. & Mahon, B. P. Adeno-associated virus serotype 2 induces cell-mediated immune responses directed against multiple epitopes of the capsid protein VP1. *J. Gen. Virol.* **90**, 2622–33 (2009).

106. Wu, T. L. *et al.* CD8+ T cell recognition of epitopes within the capsid of adeno-associated virus 8-based gene transfer vectors depends on vectors' genome. *Mol. Ther.* (2014). doi:10.1038/mt.2013.218

107. Kotterman, M. A. & Schaffer, D. V. Engineering adeno-associated viruses for clinical gene therapy. *Nat. Rev. Genet.* (2014). doi:10.1038/nrg3742

108. Gardner, M. R. *et al.* Anti-drug Antibody Responses Impair Prophylaxis Mediated by AAV-Delivered HIV-1 Broadly Neutralizing Antibodies. *Mol. Ther.* (2019). doi:10.1016/j.ymthe.2019.01.004

SHUHAO XIAO

Date of Birth: 05/27/1995
Location of Birth: Wuhan, Hubei Province,
People's Republic of China

EDUCATION

Johns Hopkins Bloomberg School of Public Health — Baltimore, MD
Master of Science (Sc.M) in Molecular Microbiology and Immunology — Expected 2019
Thesis advisor: Professor Prakash Srinivasan
Thesis title: "Engineering a self-targeting entry inhibitor for malaria prophylaxis"

South University of Science and Technology of China — Shenzhen, China
Bachelor of Science (B.S.) in Biology — 2017

EXPERIENCE

Johns Hopkins Bloomberg School of Public Health — Baltimore, MD
Graduate Researcher — 2017 – Present
Supervisor: Professor Prakash Srinivasan

(1) Engineering a novel immunoglobulin fusion protein RON2L-Ig that blocks malaria parasite Plasmodium falciparum invasion into host cells, and (2) employing adeno-associated viral (AAV) vectored immuno-prophylaxis system to deliver the gene of inhibitor RON2L-Ig in a mouse model.

Beijing Genomics Institute at China National GeneBank — Shenzhen, China
Intern/Research Assistant — 2016 – 2017
Supervisor: Dr. Xiao Liu

Gene co-expression network analysis of single-cell RNA sequencing (scRNA-seq) data of regulatory T cells (Tregs) to identify unreported subsets and driver genes.

The Henry Samueli School of Engineering at University of California, Irvine — Irvine, CA
Visiting Student — Summer, 2016
Supervisor: Professor Chenyang Sunny Jiang

Computational modeling the risk of Staphylococcus aureus skin infection for crews aboard the International Space Station using Monte-Carlo simulation.

South University of Science and Technology of China — Shenzhen, China
Undergraduate researcher — 2015 - 2017
Supervisor: Professor Tao Wang

Structural characterization of Mycobacterium tuberculosis protein mycobacterial proteasomal adenosine tri-phosphatase (Mpa) using X-ray crystallography.